



THESIS APPROVAL
GRADUATE SCHOOL, KASETSART UNIVERSITY

Master of Science (Chemistry)

DEGREE

Chemistry

FIELD

Chemistry

DEPARTMENT

TITLE: Kinetic Study of HIV-1 Reverse Transcriptase Complexed with Novel Inhibitors Based on Fluorometric Measurement and Molecular Docking Calculations

NAME: Miss Ratsupa Thammaporn

THIS THESIS HAS BEEN ACCEPTED BY

THESES ADVISOR

(Associate Professor Supa Hannongbua, Dr.rer.nat.)

THESES CO-ADVISOR

(Associate Professor Supanna Techasakul, Ph.D.)

THESES CO-ADVISOR

(Assistant Professor Chak Sangma, Ph.D.)

THESES CO-ADVISOR

(Assistant Professor Kiattawee Choowongkomon, Ph.D.)

DEPARTMENT HEAD

(Assistant Professor Noojaree Prasitpan, Ph.D.)

APPROVED BY THE GRADUATE SCHOOL ON _____

DEAN

(Associate Professor Gunjana Theeragool, D.Agr.)

THESIS

KINETIC STUDY OF HIV-1 REVERSE TRANSCRIPTASE
COMPLEXED WITH NOVEL INHIBITORS BASED ON
FLUOROMETRIC MEASUREMENT AND MOLECULAR DOCKING
CALCULATIONS

RATSUPA THAMMAPORN

A Thesis Submitted in Partial Fulfillment of
the Requirements for the Degree of
Master of Science (Chemistry)
Graduate School, Kasetsart University
2009

Ratsupa Thammaporn 2009: Kinetic Study of HIV-1 Reverse Transcriptase Complexed with Novel Inhibitors Based on Fluorometric Measurement and Molecular Docking Calculations. Master of Science (Chemistry), Major Field: Chemistry, Department of Chemistry. Thesis Advisor: Associate Professor Supa Hannongbua, Dr.rer.nat.
79 pages.

Currently, HIV infection is an important problem in the worldwide. The rate of infected patients is very high and increase every year. The mutation of HIV-1 reverse transcriptase (HIV-1 RT) reduces the efficient inhibition of anti-AIDS drugs. Accordingly, novel inhibitors are developed to inhibit HIV-1 RT. The objective of this work is to develop biological testing of novel HIV-1 RT inhibitor by using fluorometric measurement. Expression and purification of the wild-type HIV-1 RT were produced from the recombinant bacteria. The yield of HIV-1 RT in culture 1 liter was 14.06 mg. The efficiency of the purified HIV-1 RT was comparable to the commercial HIV-1 RT. The inhibition of nevirapine and dipyrindiazepinone derivatives on the enzymatic activity of the wild-type HIV-1 RT was investigated using a fluorometric measurement. From screening with 1 μ M dipyrindiazepinone derivatives, inhibition of HIV-1 RT activity with compounds namely, NA14, NA15, NA16, NA17 and 68NV was found to be higher efficiency than nevirapine. The IC_{50} value of nevirapine was 15.67 μ M which is layed in the range of reported by the other groups. Therefore, the fluorometric method can be successfully applied for inhibiting studies of HIV-1 RT activity. In addition, the dipyrindiazepinone derivatives, NA14 and NA15 were shown the best inhibiting efficiency for the wild-type HIV-1 RT among other derivatives with IC_{50} values of 0.2138 and 0.5199 μ M, respectively. Furthermore, the molecular docking was used to study the orientations of inhibitors in HIV-1 RT binding pocket by using GOLD program with GoldScore and ChemScore fitness functions. The results indicate that the ChemScore fitness function is suitable to consider the docked orientations. The thiophenyl side chains of NA14 and NA15 interact with residues such as Lys103, Val106, Phe227, Leu234, His235, Pro236 and Tyr318. The present of methyl group at R_1 position interact with Trp229. Moreover, the methoxy group at the thiophenyl side chain of NA15 generated H-bonding with backbone of residue Val106 with 2.86 Å.

Student's signature

Thesis Advisor's signature

/ /

ACKNOWLEDGEMENTS

First, I would like to thank my advisor, Associate Professor Supa Hannongbua for her kindness, valuable suggestions, encouragement, continuous support and constant inspiration the course of my degree. I would sincerely like to thank Assistant Professor Kiattawee Choowongkomon for kindly providing valuable suggestions and helpful guidance. I also wish to express my appreciation to Associate Professor Supanna Techasakul and Assistant Professor Chak Sangma for valuable suggestions and comments to make my thesis complete.

I am deeply appreciated to Dr. Patchreenart Saparpakorn who took the time to help and suggest in my thesis. Furthermore, I am also grateful to Mr. Kun Silprasit who I spent time discussing in my experimental work.

This work was supported in part by the Thailand Research Fund (RTA5080005), the National Center of Excellence in Petroleum, Petrochemicals Technology and Advanced Materials, NCE-PPAM) and National Synchrotron Research Center, Thailand.

Special thanks are due to University of Vienna and the High Performance Computing Center of National Electric and Computer Technology (NECTEC) in providing SYBYL. The Laboratory for Computational and Applied Chemistry (LCAC) at Kasetsart University are also greatfully acknowledge for computational resource and software facilities. I would like to thank Department of Biochemistry at Kasetsart University for providing experimental research facilities.

I appreciate my colleagues at LCAC and Biochemistry Department for their helpful assistance and supporting during my study. Finally, I would like to thank my parents and my brother, who encouraged me to achieve success in my education.

Ratsupa Thammaphorn

October, 2009.

TABLE OF CONTENTS

	Page
TABLE OF CONTENTS	i
LIST OF TABLES	ii
LIST OF FIGURES	iv
LIST OF ABBREVIATIONS	vii
INTRODUCTION	1
OBJECTIVES	5
LITERATURE REVIEW	6
MATERIALS AND METHODS	18
Materials	18
Methods	23
RESULTS AND DISCUSSION	30
CONCLUSIONS	52
LITERATURE CITED	54
APPENDICES	60
Appendix A IC ₅₀ determination from fluorometric assay	61
Appendix B Poster Presentation to Conferences	75
CURRICULUM VITAE	78

LIST OF TABLES

Table	Page
1 The structures of dipyrindodiazepinone derivatives	4
2 Quantity of reagent used for preparation of SDS-PAGE	20
3 Concentration of stock solution of dipyrindodiazepinone derivatives	27
4 Purification table and specific activity measured with the fluorometric method	32
5 Percent inhibition from three independent experiments in each dipyrindodiazepinone derivative at 1 μ M. Fold relative inhibition are shown in comparison to nevirapine	36
6 GoldScore and ChemScore of docked 68NV derivatives compared with 68NV in HIV-1 RT (PDB code 1KLM)	46
7 GoldScore and ChemScore of docked nevirapine derivatives and nevirapine in HIV-1 RT (PDB code 1VRT)	46
 Appendix Table	
A1 Fluorescence intensity and percent inhibition in each concentration of nevirapine	63
A2 Values from calculation of nevirapine using Nonlinear regression curves to fit to three-parameter logistic equation	64
A3 Fluorescence intensity and percent inhibition in each concentration of 68NV	65
A4 Values from calculation of 68NV using Nonlinear regression curves to fit to three-parameter logistic equation	66
A5 Fluorescence intensity and percent inhibition in each concentration of NA14	67

LIST OF TABLES (Continued)

Appendix Table		Page
A6	Values from calculation of NA14 using Nonlinear regression curves to fit to three-parameter logistic equation	68
A7	Fluorescence intensity and percent inhibition in each concentration of NA15	69
A8	Values from calculation of NA15 using Nonlinear regression curves to fit to three-parameter logistic equation	70
A9	Fluorescence intensity and percent inhibition in each concentration of NA16	71
A10	Values from calculation of NA16 using Nonlinear regression curves to fit to three-parameter logistic equation	72
A11	Fluorescence intensity and percent inhibition in each concentration of NA17	73
A12	Values from calculation of NA17 using Nonlinear regression curves to fit to three-parameter logistic equation	74

LIST OF FIGURES

Figure		Page
1	The HIV-1 life cycle	8
2	The structure of the HIV-1 RT heterodimer. The polypeptide backbones of the HIV-1 RT catalytic complex (Huang et al., 1998) are represented as ribbons and coils. The subunits of p51 and p66 subdomains are indicated as F (fingers), P (palm), T (thumb) and C (connection) and are represented in blue, green, yellow and red respectively. The RNaseH domain is colored purple. The dsDNA has the template in green (T) and the primer in yellow (P). The catalytically important residues of the polymerase and RNaseH active sites are shown as grey spheres. The orange spheres represent NRTI resistance mutation sites. A nevirapine molecule represented as a space filling model, colored in brown, marks the position of the NNRTI site, with associated resistance mutations for this drug class shown as purple spheres.	9
3	Structures of the nucleoside reverse transcriptase inhibitors (NRTIs)	11
4	Structures of the non-nucleoside reverse transcriptase inhibitors (NNRTIs)	12
5	Structure of the dipyrindodiazepinone compound	13
6	The steps of expression and purification of HIV-1 RT	31
7	SDS-PAGE of each purification step of <i>E.coli.</i> expressed HIV-1 RT	32
8	Standard curve of known concentration of HIV-1 RT (commercial enzyme)	33

LIST OF FIGURES (Continued)

Figure		Page
9	Time-dependent of HIV-1 RT activity in the case of 30 ng/μl of purified HIV-1 RT (▲) and 0.5 U/μl commercial HIV-1 RT (◆)	34
10	Time-dependent of inhibition of 30 ng/μl purified HIV-1 RT activity with no inhibitor (◆), nevirapine (■) and 68NV (▲)	35
11	Fold relative inhibition in comparing to nevirapine with different dipyrindiazepinone derivatives at 1 μM on the purified HIV-1 RT activity	36
12	Fold relative inhibition in comparing to nevirapine with different dipyrindiazepinone derivatives at 1 μM on the different HIV-1 RT activity. Gray bars represent 0.5 U/μl commercial HIV-1 RT. Brown bars represent 30 ng/μl purified HIV-1 RT.	37
13	IC ₅₀ values of nevirapine, 68NV and dipyrindiazepinone derivative on the enzymatic activities of HIV-1 RT. Dose-response curves were fitted to three parameter logistic equation. IC ₅₀ and standard error were reported.	39
14	The structure of the HIV-1 RT heterodimer in complex with nevirapine (atom-type color) (PDB code 1VRT)	42
15	The structure of the HIV-1 RT heterodimer in complex with delarvidine (atom-type color) (PDB code 1KLM)	42
16	Orientation of nevirapine in HIV-1 RT binding pocket (PDB code 1VRT). (a) Geometries obtained from X-ray (yellow color) and docking (atom-type color) using GoldScore fitness function. (b) Geometries obtained from X-ray (yellow color) and docking (atom-type color) using the ChemScore fitness function	43

LIST OF FIGURES (Continued)

Figure		Page
17	Orientation of delarvidine in HIV-1 RT binding pocket (PDB code 1KLM). (a) Geometries obtained from X-ray (yellow color) and docking (atom-type color) using GoldScore fitness function. (b) Geometries obtained from X-ray (yellow color) and docking (atom-type color) using the ChemScore fitness function	44
18	Superimpositions of 68NV (yellow) compared with (a) orientations of N15 (orange), N16 (green), NA15 (blue), NA16 (red) and NA17 (pink) and (b) orientations of N14 (purple) and NA14 (gray) using the GoldScore fitness function	47
19	Superimpositions of 68NV (yellow) compared with (a) orientations of N15 (orange), N16 (green), NA15 (blue), NA16 (red) and NA17 (pink) and (b) orientations of N14 (purple) and NA14 (gray) using the ChemScore fitness function	48
20	Superimpositions of nevirapine (yellow) compared with orientation of NB17 (green) and NB18 (pink) using (a) GoldScore and (b) ChemScore fitness function	49

LIST OF ABBREVIATIONS

Å	=	Angstrom
AIDS	=	Acquired immunodeficiency syndrome
Ala (A)	=	Alanine
Asn (N)	=	Asparagine
Asp (D)	=	Aspartic acid
a.u.	=	Arbitrary units
AZT	=	Azidothymidine
BSA	=	Bovine serum albumin
°C	=	Degree Celsius
Cys (C)	=	Cysteine
Da	=	Dalton
DAPI	=	4',6'-diamidino-2-phenylindole
DEAE	=	Diethylaminoethyl cellulose
dsDNA	=	Double stranded DNA
<i>E. Coli</i>	=	<i>Escherichia coli</i>
EDTA	=	Ethylenediaminetetraacetic acid disodium salt
FDA	=	The U.S. Food and Drug Administration
Gly (G)	=	Glycine
HAART	=	Highly active anti-retroviral therapy
His (H)	=	Histidine
HIV	=	Human immunodeficiency virus
HIV-1 RT	=	HIV-1 reverse transcriptase
HQSAR	=	Halogram quantitative structure-activity relationships
IC ₅₀	=	50% inhibitory concentration
IPTG	=	Isopropyl β-D-1-thiogalactopyranoside
kDA	=	Kilodalton
LB	=	Luria-Bertani broth
Leu (L)	=	Leucine
Lys (K)	=	Lysine

LIST OF ABBREVIATIONS (Continued)

mM	=	Millimolar
mRNA	=	Messenger RNA
mg	=	Milligram
ng	=	Nanogram
NNRTIs	=	Non-nucleoside reverse transcriptase inhibitors
NRTIs	=	Nucleoside reverse transcriptase inhibitors
OD	=	Optical density
PDB	=	Protein Data Bank
Phe (F)	=	Phenylalanine
Pro (P)	=	Proline
rmsd	=	Root mean square deviation
Rnase H	=	ribonuclease H
S.D.	=	Standard deviation
SDS	=	Sodium dodecyl sulfate
SDS-PAGE	=	Sodium Dodecyl Sulfate-Polyacrylamide Gel Electrophoresis
SPR	=	Surface plasmon resonance
ssRNA	=	Single stranded RNA
TEMED	=	Tetramethylethylenediamine
Trp (W)	=	Tryptophan
Tyr (Y)	=	Tyrosine
U	=	Unit
µg	=	Microgram
µl	=	Microliter
µM	=	Micromolar
v/v	=	Volumn by volumn
w/v	=	Weight by volumn

KINETIC STUDY OF HIV-1 REVERSE TRANSCRIPTASE COMPLEXED WITH NOVEL INHIBITORS BASED ON FLUOROMETRIC MEASUREMENT AND MOLECULAR DOCKING CALCULATIONS

INTRODUCTION

Human immunodeficiency virus (HIV) causes the acquired immunodeficiency syndrome (AIDS) which was originated in Africa and first appeared the first in United States in 1983. AIDS epidemic is an important problem that affects many people particularly in the third-world countries. The virus is transmitted from one person to others through blood or fluid exchanges. Then, the virus attacks white blood cells, making them lose ability to inhibit the disease. As a result, AIDS patients die owing to the HIV infections. The rate of infected patients is very high. Ten millions people worldwide infected it and died from this disease.

HIV-1 reverse transcriptase (HIV-1 RT) is a crucial enzyme which catalyzes in the conversion of single stranded RNA (ssRNA) into double stranded DNA (dsDNA). After that, the dsDNA is integrated into the host cell genome. Therefore, the role of HIV-1 RT in the HIV-1 life cycle is an interesting target for anti-AIDS highly active anti-retroviral therapy (HAART) (Spallarossa *et al.*, 2008). Two classes of HIV-1 RT drugs; nucleoside reverse transcriptase inhibitors (NRTIs) and non-nucleoside reverse transcriptase inhibitors (NNRTIs) are used to inhibit HIV-1 RT. The NRTI such as azidothymidine (AZT), which can bind to the active site of HIV-1 RT, was the basic of AIDS therapy. Furthermore, the HIV-1 RT can be blocked by NNRTIs which are noncompetitive inhibitors such as TIBO, nevirapine and efavirenz (De Jonge *et al.*, 2005).

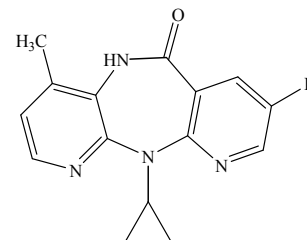
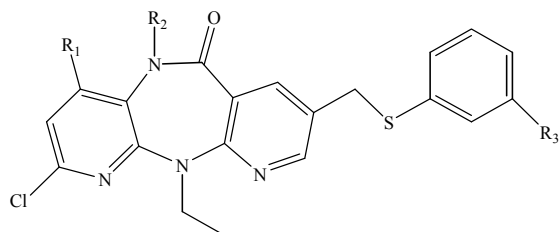
The NNRTIs are important anti-AIDS drugs for treating patient that are used in combination therapy with the nucleoside/nucleotide RTIs and protease inhibitors. The NNRTIs bind to an allosteric site located about 10 Å away from the catalytic site

of HIV-1 RT. The effect of conformational change of HIV-1 RT by binding to NNRTI will disrupt catalytic site and block DNA polymerase activity. As a result, HIV-1 RT is an inactive form and its efficiency decrease. NNRTIs have shown to be specific and toxic less than NRTIs. Accordingly, NNRTIs are an interesting inhibitor for development of a novel anti-HIV-1 inhibitor (Barreca *et al.*, 2005). Currently, there are three NNRTIs namely, nevirapine, delavirdine and efavirenz which have been approved by the U.S. Food and Drug Administration (FDA). However, the efficiencies of these inhibitors are limited by mutations of enzyme at different position such as K103N, Y181C and V106A. Therefore, the new potent compounds of NNRTIs are developed and designed to effectively inhibit the replication of HIV-1 RT both the wild type and mutant types. New anti-AIDS drug candidates, etravirine (TMC125-R165335), GW678248, YM-215389, dapivirine (TMC-120) and rilpivirine (TMC278-R278474), are effective NNRTIs against a wide range of existing drug-resistant HIV-1 viral variants (Das *et al.*, 2005; Das *et al.*, 2008; Herschhorn *et al.*, 2008).

Currently, an interaction of binding pocket of HIV-1 RT with NNRTIs is widely studied by using the computational drug design. The computational chemistry calculations have provided not only the details of molecular interaction and shape of 3D structure to determine the molecular function, but also give the useful informations about reaction and mechanism of enzyme, hydrogen bondings, polarization effects, spectra, ligand binding and biological data. There are many methods that have been applied to study interaction between binding pocket HIV-1 RT and NNRTIs such as 3D-QSAR, ONIOM, Molecular Dynamics simulations, Monte-Carlo simulations and Molecular Docking (Hannongbua, 2006). Generally, molecular docking has been used to investigate an orientation of ligand in binding pocket and binding energy values between ligand and enzyme. Therefore, this method has been used for calculating the complex of NNRTIs with HIV-1 RT in the both of wild type and mutant type to obtain information and compare with experimental data.

Furthermore, the understandable some detailed chemical mechanisms of polymerization and HIV-1 RT complexed with inhibitor are the knowledge of the kinetic parameters for an interaction between the HIV-1 RT with primer/template and nucleotides analog or non-nucleoside inhibitors that are very important to study (Pelsika & Benkovic, 1992). The important evidence of the interaction between NNRTIs and HIV-1 RT is 50% inhibitory concentration (IC_{50}) or concentration required to inhibit HIV-1 RT activity by 50%. The determination of DNA at low concentrations is challenging and interesting. There are many techniques for detecting and quantifying small amounts of DNA to determine kinetic parameters. Nowadays, fluorometric measurement can be used to analyze the quantity of dsDNA at low concentration. This method is a simple, potential and sensitive more than absorbance measurements. Fluorescence-labeled can be used to investigate interaction of RT with primer/template and nucleotides analog or non-nucleoside inhibitors which is shown in form of fluorescence intensity (Divita *et al.*, 1993).

There are many fluorophores in fluorometric measurement; for example ethidium bromide, Hoechst 33258, PicoGreen, and SYBR Green I. Each fluorophore can be used in different situations to advantage or hindrance (Rengarajan *et al.*, 2002). In this work, PicoGreen reagent was used to study the interaction of HIV-1 RT with dipyrroldiazepinone derivatives. PicoGreen reagent can detect RNA-DNA heteroduplexes formed. The fluorescence enhancement of PicoGreen is very high and little background occurs. PicoGreen is very stable to photobleaching, allowing longer exposure times and assay flexibility (Ahn *et al.*, 1996). Therefore, interaction of HIV-1 reverse transcriptase complexed with non-nucleoside reverse transcriptase inhibitors will be investigated by fluorometric measurement using PicoGreen dye. IC_{50} obtained from experiments will be compared with Molecular Docking calculations. The structures of dipyrroldiazepinone derivatives for studying inhibition of HIV-1 RT are shown in Table 1.

Table 1 The structures of dipyrindiazepinone derivatives.

Compounds	R ₁	R ₂	R ₃
68NV	H	CH ₃	H
N14	H	H	H
N15	H	H	OCH ₃
N16	H	H	F
NA14	CH ₃	H	H
NA15	CH ₃	H	OCH ₃
NA17	CH ₃	CH ₃	H
NA16	CH ₃	CH ₃	OCH ₃

Compounds	R
Nevirapine	H
NB17	NH ₃ ⁺ Cl ⁻
NB18	NH ₂

OBJECTIVES

1. To study inhibition of non-nucleoside reverse transcriptase inhibitors (NNRTIs) (nevirapine and some novel inhibitors) with HIV-1 RT by using fluorometric method.
2. To compare the inhibitory potential of NNRTI and novel inhibitors.
3. To develop of fluorescence-based assay for kinetic study of HIV-1 RT.
4. To compare of experimental and theoretical studies based on docking calculations.

LITERATURE REVIEW

Human immunodeficiency virus (HIV) is a retrovirus which causes the acquired immunodeficiency syndrome (AIDS). When patients infected HIV, the virus enters blood fluid and attacks white blood cells. There are many steps in the life cycle of HIV-1 as shown in Figure 1. The first step, the viral envelope glycoprotein, gp120 binds to the receptor on surface of target cell, CD4 and fuses into the host cells. Then, RNA and enzyme are released to the host cells. The second step, the HIV-1 reverse transcriptase (HIV-1 RT) catalyzes in the conversion single stranded RNA (ssRNA) into double stranded DNA (dsDNA). The third step, dsDNA is integrated into the host cell genome which catalyzes by the enzyme integrase in HIV-1. The integrated DNA is transcribed into messenger RNA (mRNA). Then mRNA is translated into viral proteins. The enzyme protease cleaves the viral proteins to form the functional viral proteins. The finally, the new viral RNA and viral proteins assemble into a new viral (Jonckheere *et al.*, 2000; Debnath, 2005). In process of HIV-1 life cycle, the reverse transcriptase, integrase and protease are an important enzyme for studying and designing anti-HIV-1 drug.

Reverse transcription which is accomplished by reverse transcriptase, is a crucial step of HIV life cycle. HIV-1 reverse transcriptase (HIV-1 RT) is a multifunctional enzyme which catalyzes the conversion of single-stand viral RNA into dsDNA. This process was firstly reported by Baltimore, Temin and Mizutani for RNA tumor viruses (Jonckheere *et al.*, 2000). The catalytic activities of HIV-1 RT have RNA-dependent DNA polymerase activity to form RNA/DNA hybrids, ribonuclease H (RNase H) activity to cleavage the RNA stand from RNA/DNA hybrids and DNA-dependent DNA polymerase activity to form dsDNA (Ren *et al.*, 1995; Sarafianos *et al.*, 2001; Das *et al.*, 2005). The structure of HIV-1 RT is asymmetric heterodimer of two subunits that consists of 66 kDa, subunit of 560 residues (p66) and 51 kDa, subunit of 440 residues (p51). Each subunit has four subdomains, namely fingers, thumb, palm and connection. Only p66 subunit has RNaseH domain, but p51 subunit lacks this domain (Jacobso-Molina *et al.*, 1993; Ren *et al.*, 1995; Jonckheere *et al.*, 2000) (Figure 2). The polymerase active site located at

the palm domain of p66 subunit. The fingers and thumb domains of p66 subunit formed cleft to bind the template-primer. Furthermore, the thumb domain of p66 subunit could be flexible. The three aspartic acids (Asp 110, Asp 185 and Asp 186) which are residues in the palm subdomain of p66 subunit form the polymerase active site. This catalytic triad in p66 subunit is an important to catalytic activity of HIV-1 RT. The connecting subdomain of p51 subunit occluded the cleft region. As a result, the p51 subunit is more tightly packed than the p66 subunit. The p51 subunit does not involve in catalytic activities but it supports the structure of the p66 subunit in polymerase and RNaseH activities. Moreover, the palm subdomain of p66 subunit has allosteric pocket located about 10 Å away from polymerase active site. This pocket is created when binding of NNRTI to RT (Ren *et al.*, 1995, 2008; Jonckheere *et al.*, 2000; Das *et al.*, 2005).

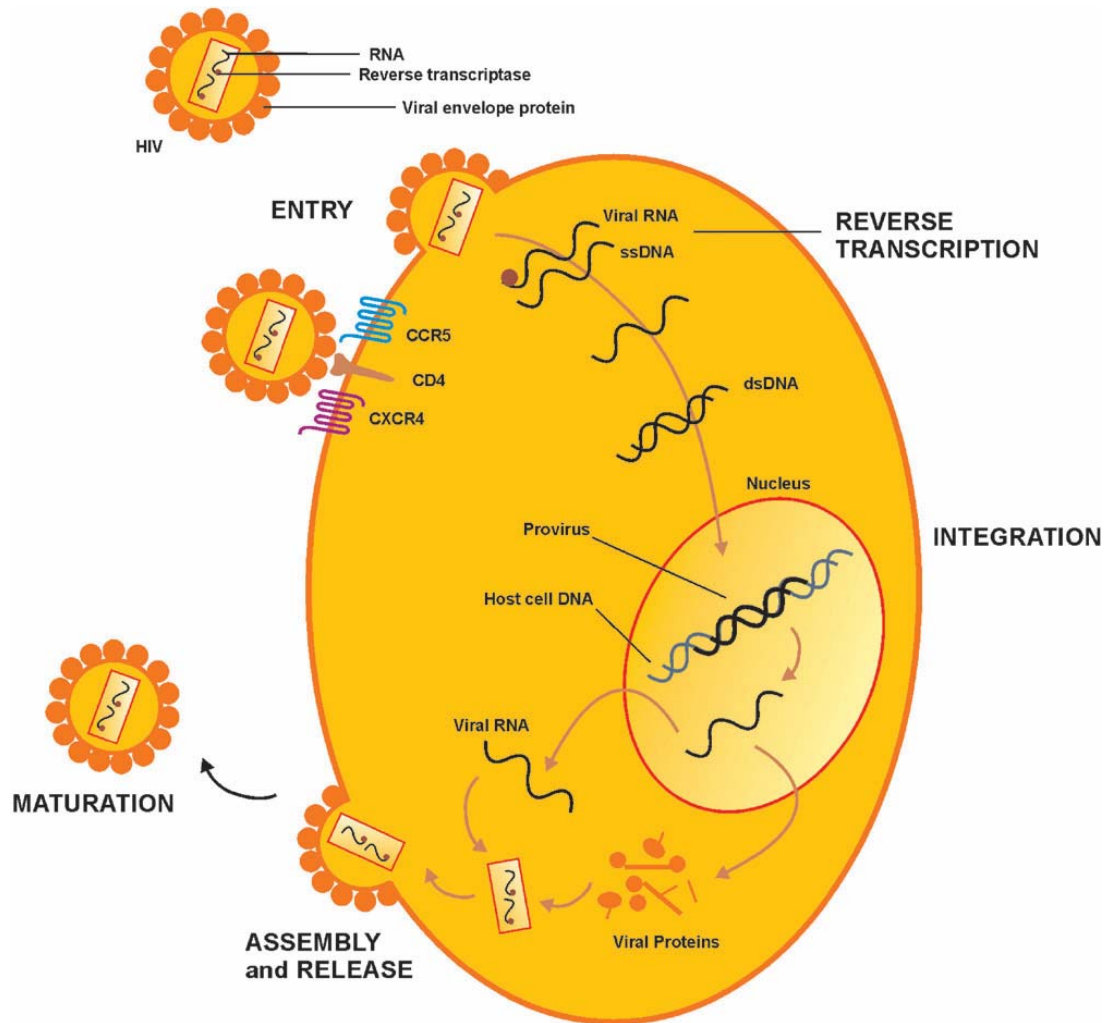


Figure 1 The HIV-1 life cycle.

Source: Busschots *et al.* (2009)

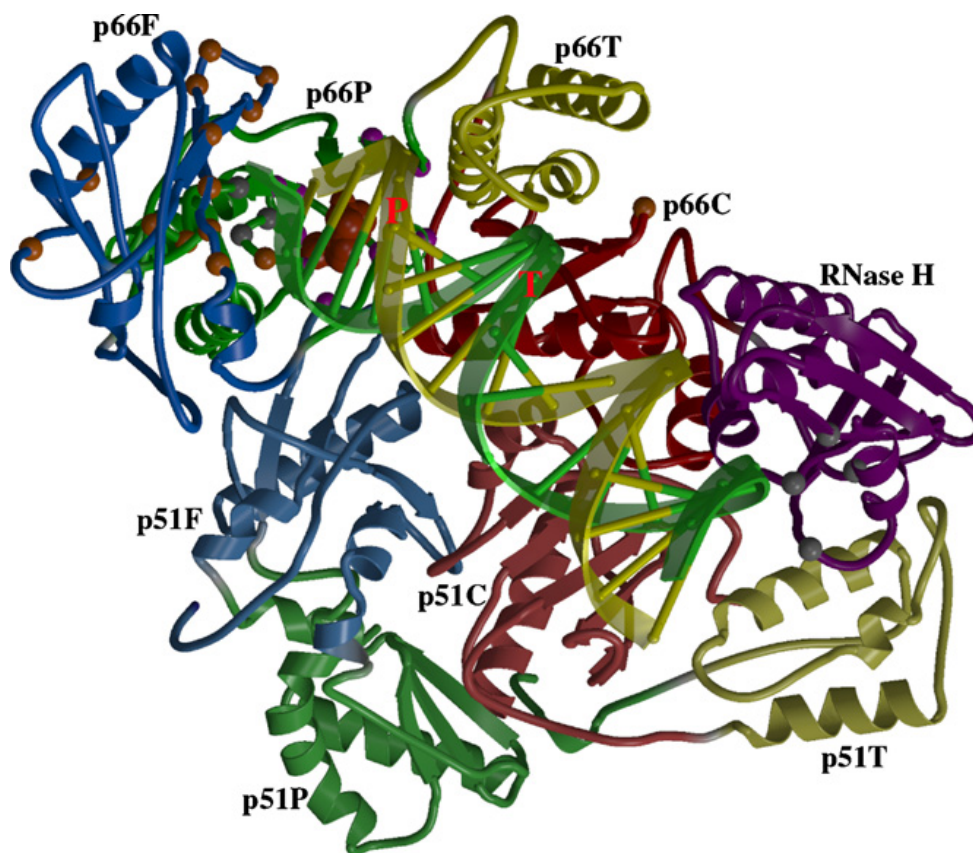


Figure 2 The structure of the HIV-1 RT heterodimer. The polypeptide backbones of the HIV-1 RT catalytic complex (Huang et al., 1998) are represented as ribbons and coils. The subunits of p51 and p66 subdomains are indicated as F (fingers), P (palm), T (thumb) and C (connection) and are represented in blue, green, yellow and red respectively. The RNaseH domain is colored purple. The dsDNA has the template in green (T) and the primer in yellow (P). The catalytically important residues of the polymerase and RNaseH active sites are shown as grey spheres. The orange spheres represent NRTI resistance mutation sites. A nevirapine molecule represented as a space filling model, colored in brown, marks the position of the NNRTI site, with associated resistance mutations for this drug class shown as purple spheres.

Source: Ren *et al.* (2008)

There are two classes of HIV-1 RT drugs that are nucleoside reverse transcriptase inhibitors (NRTIs) and non-nucleoside reverse transcriptase inhibitors (NNRTIs). NRTI is a basic of AIDS therapy for inhibiting the HIV-1 RT function. NRTIs are competitive substrate inhibitor which its structure is similarly to the structure of deoxynucleotide in nature but NRTIs lack 3' –OH group on the deoxyribose sugar/pseudosugar. For clinical use, eight NRTIs have been approved, namely 2',3-dideoxyinosine (ddI), 2',3-dideoxycytidine (ddC), (–)- β -2',3'-dideoxy-3'-thiacytidine (3TC), 5-fluoro-1-[(2R,5S)-2-(hydroxymethyl)-1,3-oxathiolan-5-yl]cytosine (FTC), (1S,4R)-4-[2-amino-6-(cyclopropyl-amino)-9H-purin-9-yl]-2-cyclopentene-1-methanolsuccinate (ABC), 3'-azido-3'-deoxythymidine (AZT) and 2',3'-deoxy-2',3'-didehydrothymidine (d4T) (Figure 3). Additionally, activity of HIV-1 RT is inhibited by NNRTIs which are small hydrophobic compounds (<600 Da) and chemically difference from nucleosides. NNRTIs are noncompetitive inhibitors which bind to the allosteric site located about 10 Å away from the catalytic site. As a result, conformation of HIV-1 RT changes to inactive form and loses efficiency of drug resistant. NNRTIs are an interesting for the development of a novel HIV-1 RT drugs because NNRTIs are specific for HIV-1 RT but no HIV-2 or other retrovirus and less toxic to cell than NRTIs. However, efficiency of NNRTIs has been limited causing from drug resistant viral strains which generated the mutation of HIV-1 RT such as L100I, K103N, V106A, Y188C/H and Y181C. For clinical use, four NNRTIs approved, namely 11-cyclopropyl-4-methyl-5,11-dihydro-6H-dipyrido[3,2-b:2',3'-e][1,4]diazepin-6-one (nevirapine), 1-[3-[(1-methylethyl)amino]-2-pyridinyl]-4-[[5]-(methylsulfonyl)amino]-1H-indol-2-yl]carbonyl]-piperazine (delavirdine), (4S)-6-chloro-4-cyclopropylethynyl-4-trifluoromethyl-1,4-dihydro-benzo[d][1,3]oxazin-2-one (efavirenz) and 4-[[6-amino-5-bromo-2-[(4-cyanophenyl)amino]-4-pyrimidinyl]oxy]-3,5-dimethylbenzotrile (etravirine) (De Jonge *et al.*, 2005; Sluis-Cremer *et al.*, 2008) (Figure 4). In clinically, NNRTIs should not be used in single drug (monotherapy) but NNRTIs were used to combine with NRTIs and protease inhibitors (De Clercq, 1997; Barreca *et al.*, 2005). But the mutation is an important problem for treating AIDS patient. Therefore, researcher has interested to develop highly effective NNRTIs. Currently, NNRTIs are the most developed that lead to the

several new RT inhibitors such as TMC-125 (etravirine), GW678248, YM-215389, TMC-120 (dapivirine) and TMC-278 (rilprvirine) (Herschhorn *et al.*, 2008).

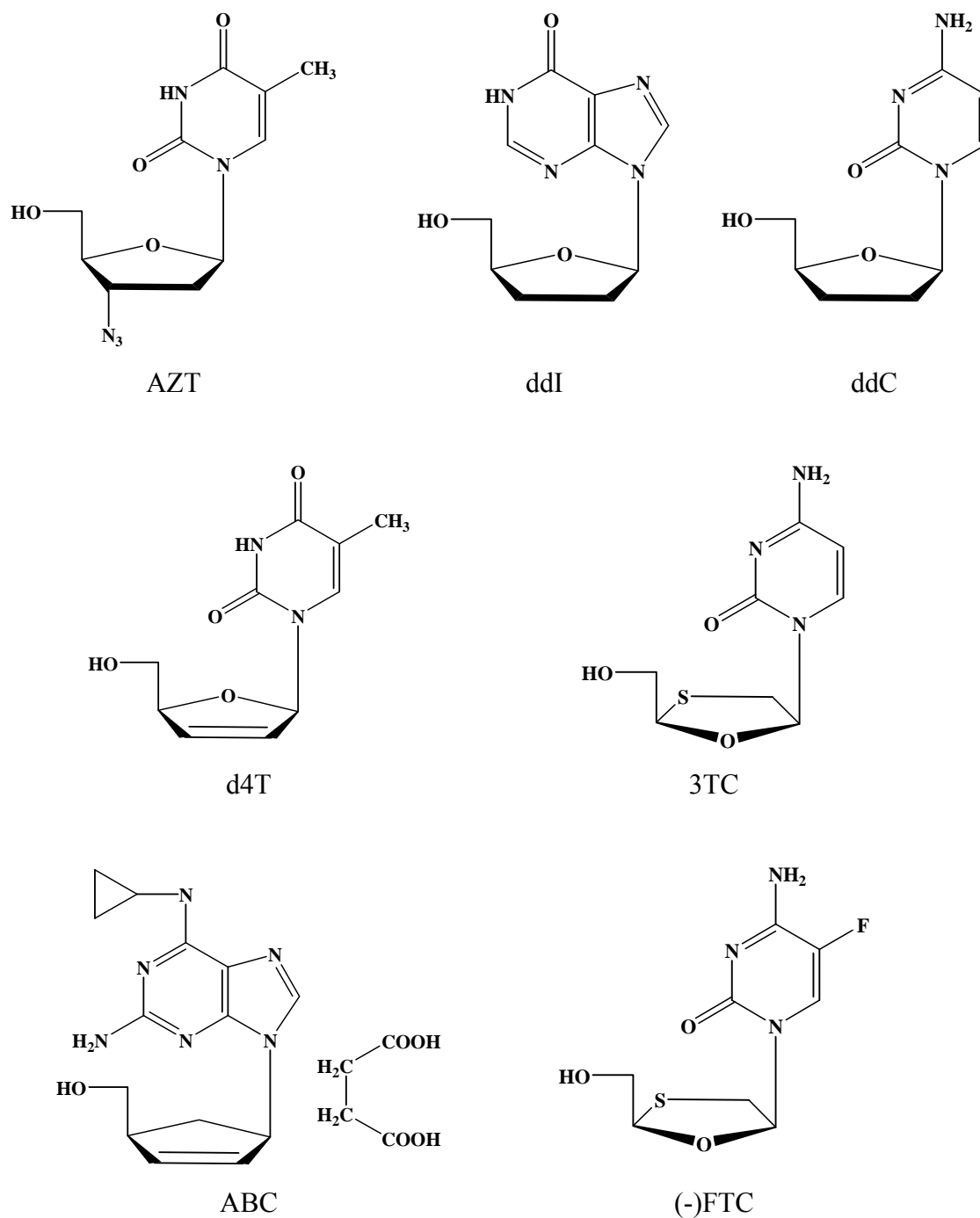
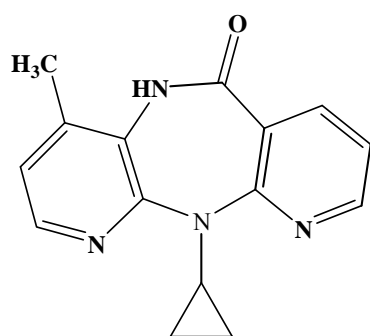
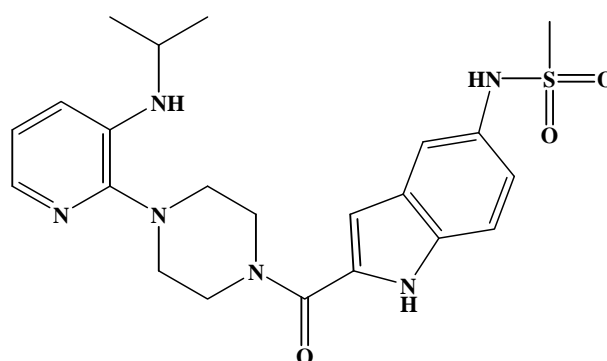


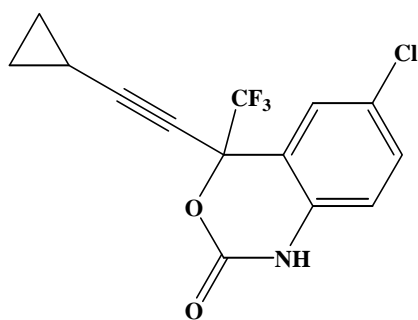
Figure 3 Structures of the nucleoside reverse transcriptase inhibitors (NRTIs).



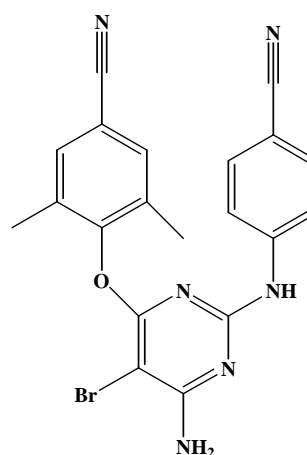
Nevirapine



delavirdine



efavirenz



etravirine

Figure 4 Structures of the non-nucleoside reverse transcriptase inhibitors (NNRTIs).

Currently, the computational chemistry calculation can be used to study interaction of HIV-1 RT with NNRTIs. For inhibitor, the surrounding amino acids are the key to determine the binding affinity. Knowledge of interaction between HIV-1 RT and NNRTIs by using the computational chemistry calculation has the benefit to design a new potential drug against both wild type and mutant type of enzyme. Methods have been used to study the interaction of NNRTI with amino acids in binding pocket of HIV-1 RT such as 3D-QSAR, ONIOM, molecular dynamics simulations, Monte-Carlo simulations and protein-based inhibitor design. Each method provides differential advantage in order to understand detail of interaction (Hannongbua, 2006). For example, in 2003, Kuno and coworker investigated interaction of nevirapine and binding site of HIV-1 RT, based on ONIOM method. In

2006, Saparpakorn and coworker designed nevirapine derivatives insensitive to the K103N and Y181C HIV-1 RT mutants by using GOLD program. In addition, Pungpo and coworker designed HIV-1 RT inhibitors by using 3D QSAR and molecular docking for studying efavirenz derivatives.

In 2003, Pungpo and coworker studied TIBO, HEPT and dipyridodiazepinone derivatives by using halogram quantitative structure-activity relationships (HQSAR) method to obtain information about common structural requirements and compare results from this method with other QSAR methods. HQSAR results indicated the similarity interactions of three derivatives of HIV-1 RT inhibitors. Comparison of HQSAR and other QSAR methods showed that HQSAR results were better than other 2D-QSAR methods to obtain information about structure of HIV-1 RT inhibitors. In particular, the predictive ability of HQSAR models from dipyridodiazepinone derivatives was indicated different features of structural requirements between WT and Y181C HIV-1 RT inhibition. The result showed that the compound, which the chlorine atom substituted at R₁ and the CH₃ group substituted at R₂, is the most active compound to inhibit wild type RT but not for Y181C HIV-1 RT inhibition, while substitution with CH₂SPh at R₃ is the highest active compound to inhibit Y181C HIV-1 RT (Figure 5).

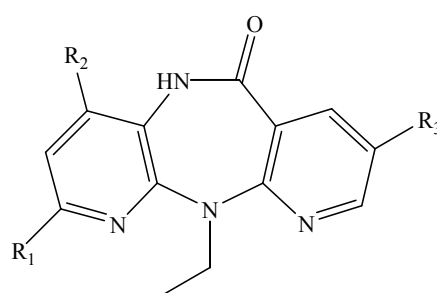


Figure 5 Structure of the dipyridodiazepinone compound.

In 2007, Khunnawutmanotham and coworker synthesized novel 2-chloro-8-arylthiomethyldipyridodiazepinone derivatives based on molecular modeling analysis against Y181C HIV-1 RT.

Molecular modeling has advantage in the investigation of the interaction of NNRTIs with HIV-RT and screening of a large library into the smaller list of effective compounds to reduce the number of compound in laboratorial test. Furthermore, knowledge of the kinetic parameters is an interesting to understand the interaction of the HIV-1 RT with primer/template and nucleotides analog or non-nucleoside inhibitors in both of detailed chemical mechanism of polymerization and the complex overall mechanism of reverse transcription (Pelsika & Benkovic, 1992). In the laboratory, the important evidence of the interaction between NNRTIs and HIV-1 RT is 50% inhibitory concentration (IC_{50}) or concentration required to inhibit HIV-1 RT activity by 50%. There are many papers reported IC_{50} values with different experiment. Nevirapine and efavirenz, approved by FDA, were used as reference in each experiment to compare with other novel inhibitors. For example, in 1990, Merluzzi and coworker found that the dipyrindodiazepinone derivatives, BI-RG-587 (nevirapine) was specific for HIV-1 RT. Moreover, BI-RG-587 has no toxicity to human cells in against HIV-1 RT. HIV-1 RT activity was assayed in the incorporation of [3H]dGTP into poly(rC):oligo(dG). They found that nevirapine could inhibit HIV-1 RT activity with IC_{50} 84 ± 4 nM.

In 1992, Balzarini and coworker studied inhibition of HIV-1 RT by TSAO-T. They found that TSAO-T could inhibit HIV-1 RT activity in the incorporation of [3H]dGTP into poly(C):oligo(dG). But in the presence of other homopolymeric template/primers, TSAO-T did not inhibited HIV-1 RT activity which contrasted with TIBO, nevirapine and HEPT derivative (I-HEPU-SdM). Nevirapine inhibited HIV-1 RT activity in the presence of poly(A):oligo(dT), poly(C):oligo(dG), poly(U):oligo(dA) and poly(I):oligo(dC) and poly(dC):oligo(dG) with IC_{50} values 23 ± 11 , 2.5 ± 0.01 , 6.5 ± 0.4 , 34 ± 6.7 and 12 ± 2.1 μ M.

In 2007, Nissley and coworker studied novel NNRTI resistance mutations of HIV-1 RT at 132 and 135 residues in p51. The purified RT, TyHRT assay and antiviral assays were used in drug resistance analyses. They found that I132M mutation could resist to nevirapine and delavirdine in high level (>10 fold) and resist to efavirenz in low level (2-3-fold). I135A and I135M mutations resisted to NNRTIs

in low level (2-fold). They reported inhibition of wild type purified RT activity with nevirapine in the incorporation of [³H]dTTP into poly(rA):oligo(dT)₁₂₋₁₈ with IC₅₀ value $7.22 \pm 1.38 \mu\text{M}$.

In the same year, Hang and coworker studied effect of fives NNRTIs (capravirine, efavirenz, GW8248, TMC-125 and nevirapine) on HIV RnaseH and DNA polymerase activities. Nevirapine inhibited DNA polymerase activity on the heteropolymeric RNA template was inhibited by nevirapine with IC₅₀ value $2.22 \mu\text{M}$. When compare with other NNRTIs, nevirapine was less potent inhibitor.

In 2008, Herschhorn and coworker used molecular modeling to screen a large chemical library against two crystal structures (PDB codes 1fk9 and 1dtq) into a smaller list of effective inhibitors. All structures in library were docked into the NNRTI binding pocket of HIV-1 RT using Surflex. The top-scoring compounds were selected for testing the efficient inhibition of HIV-1 RT activities. IC₅₀ was investigated to study interaction of NNRTIs with HIV-1 RT. The level of incorporation of [³H]dTTP into poly(rA)_n:oligo(dT)₁₂₋₁₈ template:primer was measured to study activity of HIV-1 RT. Nevirapine was used as reference with IC₅₀ $1.7 \pm 0.2 \mu\text{M}$.

The detection of quantitative DNA concentrations is an important for research. The techniques were used for measuring quantity of DNA concentrations such as absorbance method (A_{260}), isotopic methods and fluorometric measurement. Absorbance measurement at 260 nm is the most technique for determining nucleic acid concentrations. This technique is simple and easy but it can not detect small quantities of dsDNA. The assay is insensitive. The absorbance method provides the large contribution of nucleotides, ssDNA, RNA and other contaminants to the total signal which can not distinguish (Singer *et al.*, 1997; Rengarajan *et al.*, 2002). Isotopic methods for measuring HIV-1 RT activity are highly sensitive but they are many disadvantages. Firstly, laboratories that can be used to study these assay must get licenses for radioactivity. Secondly, they are time-consuming procedures. Thirdly, the disposal of radioactive isotopes which are required for these assays is a

toxic to environment (Chavan *et al.*, 1995). The fluorometric measurement is a novel approach that is a rapid, efficient and inexpensive technique. This technique is developed for HIV-1 RT activity measurement. The quantities of low concentration of dsDNA are detected using fluorometry with newer fluorophores. This method is widely used because it is simple and more sensitive than absorbance measurements. In 1995, Chavan and coworker studied and developed a novel fluorometric assay for RT activity with 4',6'-diamidino-2-phenylindole (DAPI). They have demonstrated that RT activity can be detected crude sample by fluorometric assay. Fluorometric assay is more rapid and less labor-intensive than isotopic assay for RT activity and much less expensive than nonisotopic assay that measure the incorporation of nucleotide into DNA by immunological detection method. The fluorescence intensity of this dye is enhanced which correlated to incorporation of dTTP into poly(A):oligo(dT) but in present of dsDNA did not increase fluorescence. In 1996, Seville and coworker studied fluorometric assay for DNA polymerases and reverse transcriptase, they found that fluorometric assay is quick, easy and inexpensive method for measuring the activity of replication enzymes by PicoGreen when compared with isotopic assay. In 2006, Geitmann and coworker studied the mechanism of NNRTI resistance by using surface plasmon resonance (SPR) biosensor-based method for studying the pre-steady-state kinetics of the interaction between HIV-RT and NNRTIs.

There are many fluorophores for fluorometric measurement. The binding modes of dye molecules bound with DNA are major or minor groove-binding and intercalation. Type of minor-groove binders are Hoechst 33342, Hoechst 33258 and 4',6'-diamidino-2-phenylindole (DAPI). Classes of dyes which intercalate into dsDNA are divided such as acridines, anthraquinones, cyanine dyes (PicoGreen, YOYO-1 iodide, SYBR Green I and SYBR GOLD) and phenanthridinium ions (ethidium bromide and propidium iodide) (Ihmels *et al.*, 2005). Researcher studied and developed fluorophores in quantitative determination of small amounts of dsDNA. Each fluorophore gave different qualifications. For example, the fluorescence enhancement of ethidium bromide that binds to dsDNA by intercalation is the both toxic and mutagenic. SYBR Green I has advantage because it is selectively assay

dsDNA in the presence of contaminants of RNA, ssDNA, nucleotides and protein. Moreover, it can detect DNA at low concentration, low cycle number and low target number DNA amplification products (Rye *et al.*, 1993 and Karlsen *et al.*, 1995). PicoGreen is a fluorophore which was shown intercalation to DNA (Cosa *et al.*, 2001). It has similar character to SYBR Green I for affinity which there is high affinity for DNA and a large fluorescence enhancement upon DNA binding. The fluorescence enhancement of PicoGreen is high when bound to dsDNA. But the unbound dye has a little background therefore it has no fluorescence. PicoGreen is very stable for photobleaching, allowing longer exposure times and assay flexibility (Ahn *et al.*, 1996). In 1997, Singer and coworker studied characterization of PicoGreen reagent and developed a fluorescence-based solution assay for dsDNA quantitation. They found that enhancement of fluorescence intensity of this dye upon binding dsDNA is >1000-fold. The fluorescence intensity of PicoGreen binds to poly(dA).poly(dT) and poly(dG).poly(dC) homopolymers. Its excitation and emission maxima are located near these of fluorescein. In 2002, Rengarajan and coworker compared sensitivity of several different fluorophores for measuring DNA concentrations by fluorometry. They found that SYBR Green I and PicoGreen are more sensitive for quantifying DNA concentrations than ethidium bromide and Hoechst 33258.

MATERIALS AND METHODS

Materials

1. Enzchek[®] Reverse Transcriptase Assay Kit (E-22064, Molecular Probes).

This material was contained with

- 1.1 PicoGreen dsDNA quantitation reagent, 0.55 ml of 400X dye in DMSO
- 1.2 20X TE buffer, 12 ml of 200 mM Tris-HCl, 20 mM EDTA, pH 7.5
- 1.3 Lambda DNA standard, 0.55 ml of 100 µg/ml DNA in TE buffer
- 1.4 Poly(A) ribonucleotide template (350 base long), 55 µl of 1 mg/ml template in 100 mM Tris-HCl, 0.5 mM EDTA, pH 8.1.
- 1.5 Oligo d(T)₁₆ primer, 55 µl of 50 µg/ml primer in 100 mM Tris-HCl, 0.5 mM EDTA, pH 8.1
- 1.6 Polymerization buffer, 22.5 ml of 60 mM Tris-HCl, 60 mM KCl, 8 mM MgCl₂, 13 mM DTT, 100 µM dTTP, pH 8.1
- 1.7 EDTA, 2.5 ml of a 200 mM solution in water

2. HIV-1 Reverse Transcriptase (AM2045, Applied Biosystems).

This material was contained with

- 2.1 10 U/µl of HIV-1 reverse transcriptase
- 2.2 10X RT reaction buffer, 1 ml of 500 mM Tris-HCl pH 8.3, 750 mM KCl, 30 mM MgCl₂, 50 mM DTT

3. Chemicals

- 3.1 Acetic acid (J. T. Baker, Thailand)
- 3.2 Acrylamide (Bio Basic, Canada)
- 3.3 Agar bacteriologico americano (Pronadisa, Spain)

- 3.4 Ammonium sulfate (Bio Basic, Canada)
- 3.5 Ammonium persulfate (Ajax Finechem, Australia)
- 3.6 Ampicillin
- 3.7 Bis-acrylamide (Bio Basic, Canada)
- 3.8 Bradford Reagent (Bio Rad, USA)
- 3.9 Bromophenol blue (Fisher Scientific, UK)
- 3.10 Bovine serum albumin (BSA) (Fluka Biochemika, USA)
- 3.11 Cellulose phosphate (P11 cation exchanger) (England)
- 3.12 Coomassie brilliant blue R-250 (Bio Basic, Canada)
- 3.13 Diethylaminoethyl cellulose (DEAE anion exchanger) (England)
- 3.14 Dimethyl sulfoxide (DMSO) (Labscan, Thailand)
- 3.15 Ethylenediaminetetraacetic acid disodium salt (EDTA) (Univar, Australia)
- 3.16 Glycerol (Ajax Finechem, Australia)
- 3.17 Glycine (Ajax Finechem, Australia)
- 3.18 Isopropyl β -D-1-thiogalactopyranoside (IPTG) (Fermentus, USA)
- 3.19 Lysozyme (Sigma, USA)
- 3.20 2-mercaptoethanol (Merck, Germany)
- 3.21 Methanol (Ajax Finechem, Australia)
- 3.22 Sodium dodecyl sulfate (SDS) (Bio Basic, USA)
- 3.23 Sodium chloride (J. T. Baker, Malaysia)
- 3.24 Tetramethylethylenediamine (TEMED) (Bio Basic, USA)
- 3.25 Triton[®] X-100 (USB Corporation, USA)
- 3.26 Tris (hydroxymethyl) aminomethane (Research Organic, USA)
- 3.27 Tryptone type-I (Himedia, India)
- 3.28 Yeast extract powder (Himedia, India)

4. Buffers and Solutions

4.1 Luria-Bertani (LB) broth / 1,000 ml

Tryptone	10 g
Yeast extract	5 g
NaCl	5 g

The mixture was autoclaved for 3 hours

4.2 Sodium Dodecyl Sulfate-Polyacrylamide Gel Electrophoresis (SDS-PAGE)

Table 2 Quantity of reagent used for preparation of SDS-PAGE.

Reagents	Volume of separating gel for 12% gel in 5 ml (ml)	Volume of stacking gel in 2 ml (ml)
Distilled water	1.6	1.4
30% Acrylamide	2.0	0.33
1.5 M Tris, pH 8.8	1.3	-
0.5 M Tris, pH 6.8	-	0.25
10% SDS	0.05	0.02
10% Ammonium persulfate	0.05	0.02
TEMED	0.002	0.002

The protein samples were mixed with 1X protein loading dye and boiled for 20 minutes. The electrophoresis was set in 1X running buffer at 150 volts for 1.30 hour. The gel was stained by coomassie blue R-250 in staining solution and de-stained in de-staining solution. Each reagent was prepared as followed:

30% Acrylamide (30.8% T, 2.6% C)/ 100 ml

30% Acrylamide 30 g

N,N'-methylenebisacrylamide (BIS) 0.8 g

Add distilled water to 100 ml

Separating solution (1.5 M tris, pH 8.8)/ 200 ml

Tris base 36.3 g

Adjust pH to 8.8 and add distilled water to 200 ml

Stacking solution (0.5 M tris, pH 6.8)/ 100 ml

Tris base 6 g

Adjust pH to 6.8 and add distilled water to 100 ml

10% Ammonium persulfate/ 1 ml

Ammonium persulfate 100 mg

Add distilled water to 1 ml

6X protein loading dye

0.5 M tris, pH6.8 7 ml

Glycerol 3 ml

SDS 1 g

Bromophenol blue 1.2 mg

5X running buffer/ 1000 ml

0.125 M tris base 15.1 g

0.96 M Glycine 72.0 g

0.5% w/v SDS 5 g

5X straining solution/ 500 ml

0.5% w/v coomassie blue R-250	2.5 g
40% methanol	200 ml
10% acetic acid	50 ml

5X de-straining solution/ 1000 ml

40% methanol	400 ml
10% acetic acid	100 ml

4.3 Buffer for purification protein

10X lysis buffer/ 500ml

100 mM Tris-HCl, pH 8.0	6.055 g
750 mM NaCl	21.915 g

Add distilled water to 500 ml and then dilute 10 times for using as working buffer

10X column buffer/ 500 ml

500 mM Tris-HCl, pH 7.5	26.28 g
10 mM EDTA from 500 mM EDTA	10 ml
0.5% v/v 2-mercaptoethanol	2.5 ml

Add distilled water to 500 ml and then dilute 10 times for using as working buffer

Methods

1. Expression of Reverse Transcriptase

The recombinant wild type HIV-1 RT plasmids of p51 and p66 were provided by K. Silprasit, in laboratory of Dr. K. Choowongkomon, Department of Biochemistry, Kasetsart University. The p51 and p66 plasmids were separately transformed and expressed. A single colony of bacteria containing each recombinant plasmid of p51 and p66 was cultured in 3 ml Luria-Bertani (LB) containing 100 µg/ml ampicillin and shaken at 220 rpm, 37°C overnight (about 15 hours). After that, the 3 ml starter was transferred into new flask of 500 ml LB containing 100 µg/ml ampicillin, then was cultured by shaking at 220 rpm, 37°C until the OD₆₀₀ reached 0.6-0.8. Then isopropyl β-D-1-thiogalactopyranoside (IPTG) was added with final concentration 0.4 mM in cell cultures to induce the protein expression and continued shaking at 220 rpm, 25°C overnight. The expressed protein was visualized by using the SDS-PAGE technique.

2. Purification of Reverse Transcriptase

After induction, the expressed cell cultures were harvested by centrifugation at 5000xg for 10 minutes. The pellet was suspended in 1X lysis buffer (10 mM Tris-HCl, pH 8.0 and 75 mM NaCl) containing 0.5% Triton[®] X-100. 1 mg/ml lysozyme was added and incubated with gentle shaking at 30°C for 15 minutes. After that, the mixture was sonicated for 15 minutes and centrifuged at 10,000xg for 30 minutes. The target protein in supernatant was precipitated with 30% ammonium sulfate while stirring in ice bucket for 15 minutes. The pellet was collected after centrifugation at 10,000xg for 30 minutes. After that, the pellet was dissolved in 1X column buffer (50 mM Tris-HCl pH 7.5, 1 mM EDTA, and 0.05% 2-mercaptoethanol) containing 5% glycerol and dialyzed in the same buffer, pH 9.0 at 4°C overnight. Both solution containing p51 and p66 proteins were mixed and incubated for 3 hours to obtain the active HIV-1 RT. The heterodimer of HIV-1 RT was applied to phospho-cellulose P11 column and eluted with 0.3 M NaCl in the same buffer pH 9.0. The active

protein in elutant was dialyzed in column buffer, pH 7.5 at 4°C overnight. After that the protein solution was applied to DEAE cellulose column chromatography and eluted with 0.3 M NaCl in the same buffer, pH 7.5. Then, the active fraction was concentrated with concentrator with membrane cut-off of 100 kDa. The heterodimer of HIV-1 RT was stayed in upper fraction and was stored frozen at -20°C until used. Each purified step was kept for detection by using the SDS-PAGE technique. Finally, the concentration of each purified step was determined by Bradford method.

3. Protein concentration measurement (Bradford method)

Protein concentration was measured by Bradford method. Bovine serum albumin (BSA) was a standard protein for standard curve construction. Various concentration of BSA was varied ranging from 0.2, 0.4, 0.6, 0.8 and 1 mg/ml in distilled water. Bradford reagent was diluted with distilled water in the ratio 1:4 (v/v). The 20 µl of each BSA was mixed with 1000 µl of 1:4 (v/v) diluted dyes in microcentrifuge tube 1.5 ml. The solution was incubated at room temperature for 5 min. After that, this solution was measured an absorbance at 595 nm on UV-visible spectrophotometer. The standard curve was created by plotting between the concentrations of BSA and the absorbances. The protein samples were also prepared with the same method. Thus, from this standard curve we could exactly calculate the protein concentration.

4. SDS-PAGE analysis

The protein samples were mixed with 1X protein loading dye and boiled for 20 minutes. 10 µl of each sample was loaded into the well. The electrophoresis was set in 1X running buffer at 150 volts for 1 hour. The gel was strained in a straining solution (0.5% w/v coomassie blue R-250, 40% (v/v) methanol and 10% (v/v) acetic acid) for 30 minutes and de-strained in a de-straining solution (40% (v/v) methanol and 10% (v/v) acetic acid).

5. Enzyme activity assay with fluorometric method

The mixture of 5 μ l of poly(A) ribonucleotide template and 5 μ l of oligo d(T)₁₆ primer was incubated for 1 hour at room temperature and diluted to 200 fold with polymerization buffer (60 mM Tris-HCl, 60 mM KCl, 8 mM MgCl₂, 13 mM DTT, 100 μ M dTTP, pH 8.1). PicoGreen reagent was diluted by adding into TE buffer (10 mM Tris-HCl, 1 mM EDTA, pH 7.5) with ratio 1:2000.

4 μ l of the template/primer were mixed into 2 μ l of each protein sample on ice. The mixtures were incubated at 37°C for 10 minutes. The reaction was stopped by adding 5 μ l of 200 mM EDTA and incubated on ice for 30 minutes. After that, 200 μ l of PicoGreen solution was added to reaction. Then the reaction was incubated on ice for 15 minutes by protecting the samples from light. The reaction was determined by fluorescence measurement with excitation wavelengths at 502 nm and emission wavelengths at 523 nm.

6. Purification table

The total protein of each step was determined by Bradford method. The lambda DNA was used to estimate the amount of RNA-DNA hybrids in enzyme activity determination by using the fluorometric method. Various concentration of lambda DNA was varied by using two-fold serial dilution in distilled water. After that, the PicoGreen solution was added to dilute lambda DNA and the fluorescence measurement was determined. The standard curve was generated by the plot between concentration of lambda DNA and the fluorescence intensity of each concentration. The activity of the protein sample in each purified step was determined with the fluorometric method (in step 5). The fluorescence intensity of each protein sample was calculated as amount RNA-DNA hybrids from standard curve of lambda DNA to determine enzyme activity. Specific activity was calculated from the enzyme activity divided by total protein. Purification fold was calculated from specific activity of each step divided by specific activity of cell lysate.

7. Kinetic study with the fluorometric method

7.1 Determine unit activity of purified HIV-1 RT

To create standard curve, a two-fold serial dilution of the commercial HIV-1 RT as known were diluted in 1X RT reaction buffer (50 mM tris HCl pH 8.3, 75 mM KCl, 3 mM MgCl₂, 5 mM DTT). Stock purified HIV-1 RT was diluted into 30 ng/μl of HIV-1 RT in Tris buffer (10 mM Tris HCl pH 8.0, 75 mM NaCl). The fluorometric method was determined by following in step 5. The standard curve was created by plotting between concentration (units) of commercial HIV-1 RT and fluorescence intensity. Thus, from this standard curve, the unit activity of purified HIV-1 RT was successfully calculated.

7.2 Determine time-dependent activity of HIV-1 RT

The template/primer was aliquoted for 4 μl to the well. Then, 2 μl of nevirapine and 68NV were added and mixed into the well. The used buffer for inhibitors dilution (10 mM tris HCl pH 7.4 contained 50% DMSO) was controlled. After that, 2 μl of 30 ng/μl of HIV-1 RT was added and mixed on ice. The reaction mixtures were incubated at 37°C for 0, 2.5, 5, 7.5, 10 and 15 minutes. The reaction was stopped by 5 μl of 200 mM EDTA and incubated on ice for 30 minutes before fluorescence measurement.

8. Inhibition of HIV-1 reverse transcriptase activity

8.1 Preparation of the dipyrindiazepinone derivatives

The dipyrindiazepinone derivatives were provided by S. Techasakul, Department of Science, Kasetsart University. For the stock solution, the dipyrindiazepinone derivatives were dissolved in dimethyl sulfoxide (DMSO). The concentrations of stock solutions are shown in Table 3. The stock solution was diluted as 100 fold by 10 mM tris HCl, pH 7.4 containing 50% DMSO.

8.2 Screening of dipyrindiazepinone derivatives

The 2 μ l of each 1 μ M dipyrindiazepinone derivative was added to the well. Then, 4 μ l of the template/primer were added and mixed into dipyrindiazepinone derivative in each well. After that, 2 μ l HIV-1 RT were added and mixed on ice. The mixtures were incubated at 37°C for 10 minutes. The reaction was stopped by 5 μ l of 200 mM EDTA and incubated on ice for 30 minutes. The fluorometric method was determined.

Table 3 Concentration of stock solution of dipyrindiazepinone derivatives.

Compounds	Concentration (mM)
Nevirapine	25
68NV	44
N14	25
N15	25
N16	12.5
NA14	12.5
NA15	25
NA16	10
NA17	20
NB17	50
NB18	-

8.3 IC₅₀ value determination

2 μ l of each dipyrindiazepinone derivative was varied by two-fold serial dilution to the well. Then, 4 μ l of the template/primer were added and mixed into dipyrindiazepinone derivative in each well. After that, 2 μ l of 30 ng/ μ l of HIV-1 RT were added and mixed on ice. The mixtures were incubated at 37°C for 10 minutes. The reaction was stopped by 5 μ l of 200 mM EDTA and incubated on ice for 30 minutes. The activity was determined by the fluorometric method. IC₅₀ values were

calculated from dose-response curves by using GraphPad Prism (trial version). Nonlinear regression curves were fitted to three-parameter logistic equation (equation 1).

$$Y = Bottom + \frac{(Top - Bottom)}{1 + 10^{LogIC_{50} - X}} \quad (1)$$

X was the logarithm of agonist concentration and Y was the percent inhibition as shown in equation 2.

$$\text{Percent Inhibition} = \frac{(\text{RT activity of no NNRTI} - \text{RT activity of NNRTI})}{\text{RT activity of no NNRTI}} \times 100 \quad (2)$$

9. Molecular modeling

9.1 Preparation the wild type HIV-1 RT and coordinates of Nevirapine and Delarvidine

The X-ray structures of wild type HIV-1 RT in complex with nevirapine and delarvidine were obtained from Protein Data Bank (PDB code 1VRT and 1KLM, respectively). The protein and ligand were prepared by using SYBYL 7.3 program. For protein, the ligand and water molecules were removed from each structure. All hydrogen atoms were added into the protein structure in order to set the complex to be the neutral molecule. For nevirapine and delarvidine, the atom types were assigned and hydrogen atoms were added. Finally, Gasteiger-Hückel charges were computed.

9.2 Preparation the nevirapine derivatives and 68NV derivatives

The structures of ligands were created by using nevirapine as template and modified by assigning atom types based on SYBYL 7.3 program. They were optimized by using the Powell optimization method and the Tripos force field for 100

step or until energy gradient was reached to 0.05 kcal/mol. Then, Gasteiger-Hückel charges were chosen for minimizing the complex structures.

9.3 Docking of nevirapine, delarvidine, nevirapine derivatives and 68NV derivatives

In this work, the GOLD program was used for docking studies of each compound. In order to validate the method, the nevirapine and delarvidine were docked back to its binding pocket. Then, nevirapine derivatives (NB17 and NB18) were docked into PDB code 1VRT of HIV-1 RT. 68NV derivatives (N14, N15, N16, NA14, NA15, NA16 and NA17) were docked into PDB code 1KLM of HIV-1 RT enzyme (PDB code 1KLM). The GoldScore and ChemScore fitness functions were used to analyze the binding in each docked compound. Fifteen genetic algorithm runs were setting. The orientations of each docked compound with GoldScore and ChemScore were selected to analyze the interaction of each dipyrindodiazepinone derivative in HIV-1 RT binding pocket.

RESULTS AND DISCUSSIONS

Part A: Expression and Purification of Reverse Transcriptase

The stages of expression and purification of reverse transcriptase are summarized in Figure 6 and the results of each stage are demonstrated in Figure 7, indicating 51 kDa and 66 kDa fragments on 12% SDS-polyacrylamide gel electrophoresis. Moreover, protein concentration and specific activity of each stage is shown in Table 4. The recombinant plasmids of p51 and p66 of wild type HIV-1 RT were expressed in *E. coli* under induction of 0.4 mM IPTG. The major bands in cell lysate at molecular weights of 51 kDa and 66 kDa were produced as shown in Figure 7, cell lysate. The expressed recombinant cells were lysed by sonication. The p51 and p66 proteins appeared in the soluble fractions (Figure 7, soluble fraction). The protein from soluble fraction was precipitated with 30% saturated ammonium sulfate which show the major bands of 51 kDa and 66 kDa obtained precipitants (Figure 7, 30% ammonium sulfate). The obtained protein from precipitation was dialyzed to remove ammonium sulfate salt. Each dialyzed protein solution was mixed and purified by Phosphocellulose P11 column. The heterodimer of HIV-1 RT was found in bound fraction and was eluted with 0.3 M NaCl. The major bands of bound fraction are shown in Figure 7, bound P11 column. While no detection of these two bands in the unbound fraction are shown in Figure 7, unbound P11 column. Finally, DEAE cellulose was used to obtain the purified protein. The target proteins appeared in unbound fraction (Figure 7, unbound DEAE column). From purification, an amount of 14.06 mg of the heterodimer of HIV-1 RT from 1 liter of cell culture was obtained. It was found that purification from the last step can give the highest activity of about 106 fold as compared to other steps. Moreover, the total protein in each purification step is decreased while purification fold increased. These could indicate the successful protocol for protein purification to get a pure protein. Table 4 shows the summary of all purification steps and increasing of purification folds in each step.

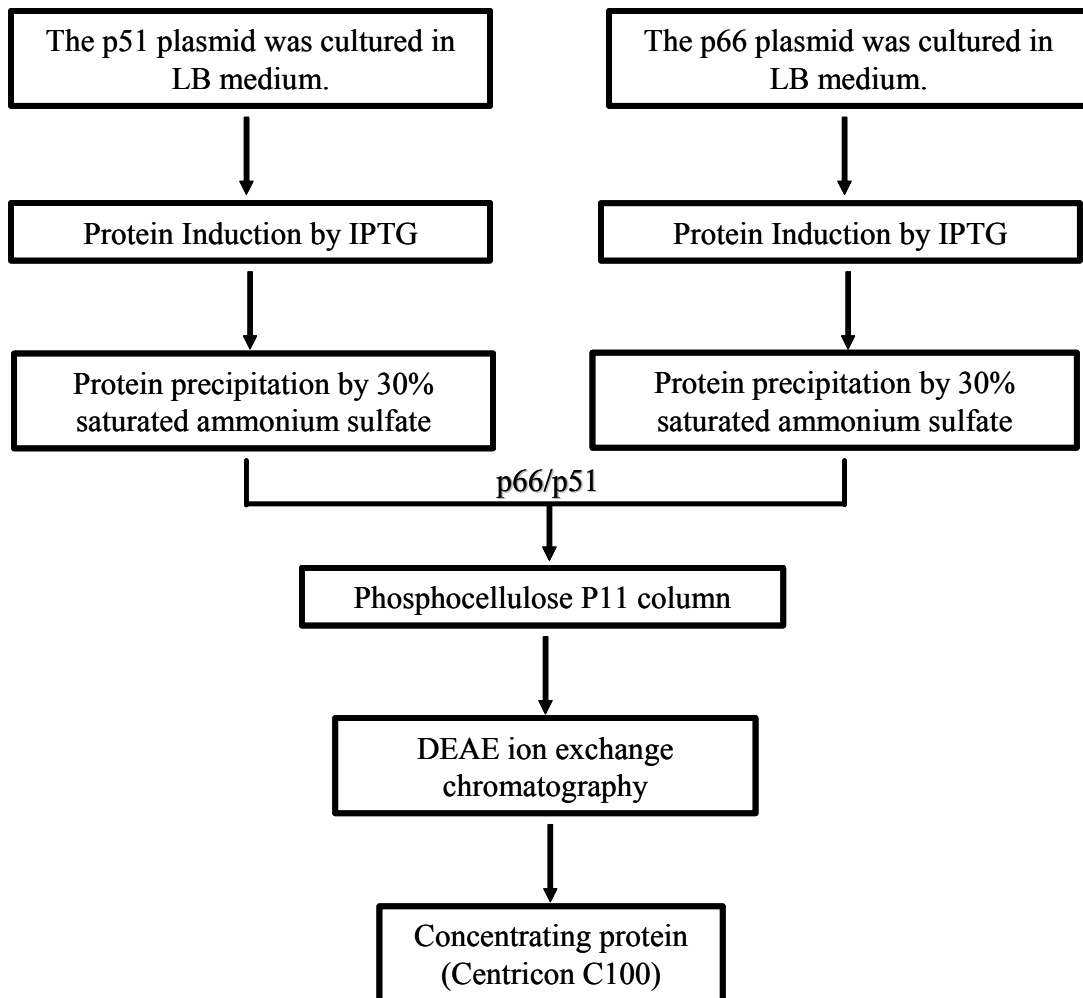


Figure 6 The steps of expression and purification of HIV-1 RT.

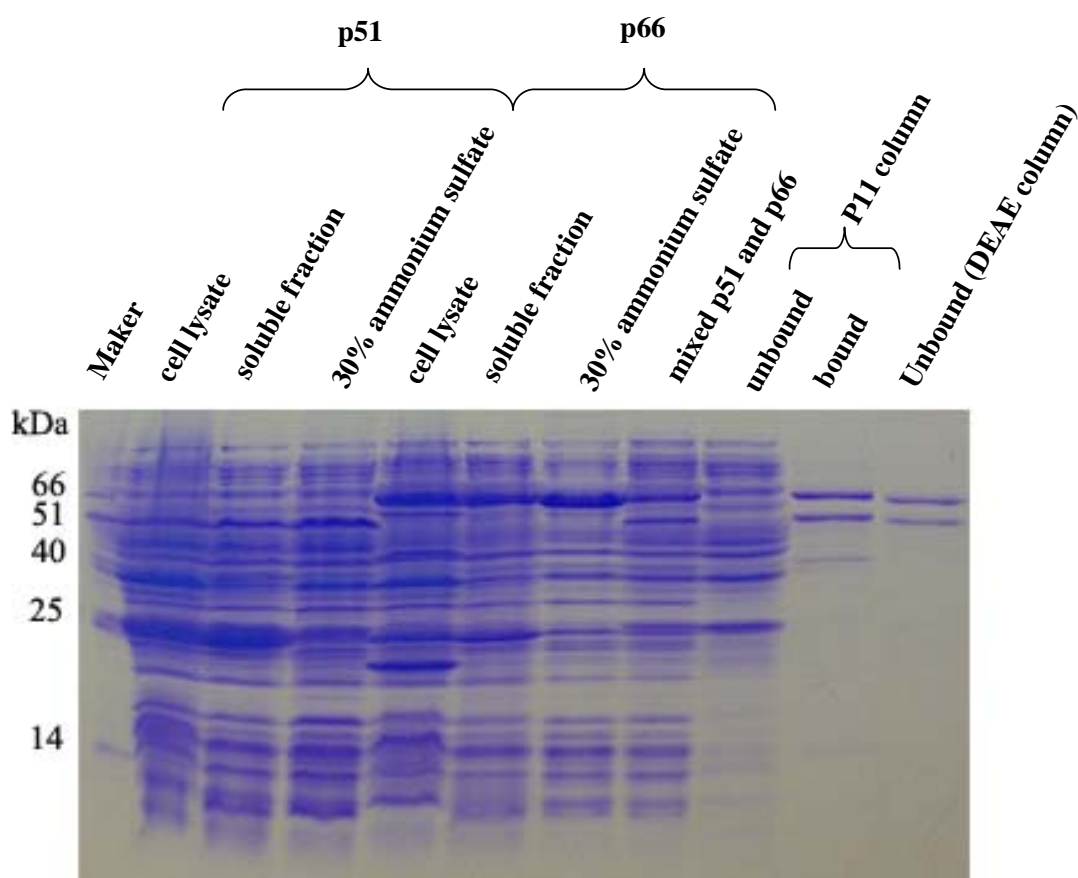


Figure 7 SDS-PAGE of each purification step of *E. coli* expressed HIV-1 RT.

Table 4 Purification table and specific activity measured with the fluorometric method.

Fraction	Total protein (mg)	Activity ($\mu\text{g}/\mu\text{l}$)	Specific activity ($\mu\text{g}/\mu\text{l}/\text{mg}$)	Fold purification
Cell lysate	332.25	2.61	0.0078	1
Soluble fraction	309.64	2.56	0.0082	1
30% ammonium sulfate	93.71	2.60	0.02	4
P11 column	46.87	6.99	0.15	19
DEAE column	14.06	11.69	0.83	106

Part B: Fluorometric assay

1. HIV-1 reverse transcriptase activity

In order to test the RT activity, the purified HIV-1 RT from the present work was compared with known concentration of a commercial HIV-1 RT (purchased from Biosystem). The activity of purified HIV-1 RT could be determined from a standard curve of serial dilutions of known concentration of the commercial HIV-1 RT in an enzyme dilution buffer. The standard curve was plotted between the fluorescence intensities and concentrations of the commercial enzyme. The fluorescence intensity of 30 ng/ μ l purified HIV-1 RT was 47.5 a.u. which was equivalent to 0.5 U/ μ l of commercial one. The result is shown in Figure 8.

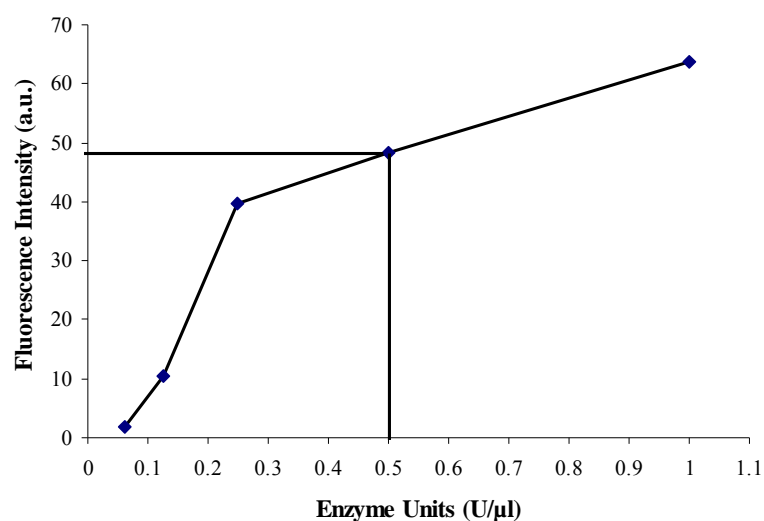


Figure 8 Standard curve of known concentration of HIV-1 RT (commercial enzyme).

Nevertheless, it was found that the fluorescence intensity increasing when increasing time. However, after 7.5 minutes the fluorescence intensity was slowly increased as shown in Figure 9. Therefore, the activity assay of HIV-1 RT was considered as a time dependent. The obtained results indicate that HIV-1 RT can generate the RNA-DNA heteroduplexes. When compared with 0.5 U/ μ l commercial

HIV-1 RT, both HIV-1 RT gave the same results in the range of 0-7.5 minutes after that the fluorescence intensity of the commercial HIV-1 RT showed higher than the purified HIV-1 RT. It indicated that the stability and activity of the commercial HIV-1 RT were better than the purified HIV-1 RT. However, both activities were not much different. Therefore, the purified HIV-1 RT can be used in further studying inhibition of HIV-1 RT activity.

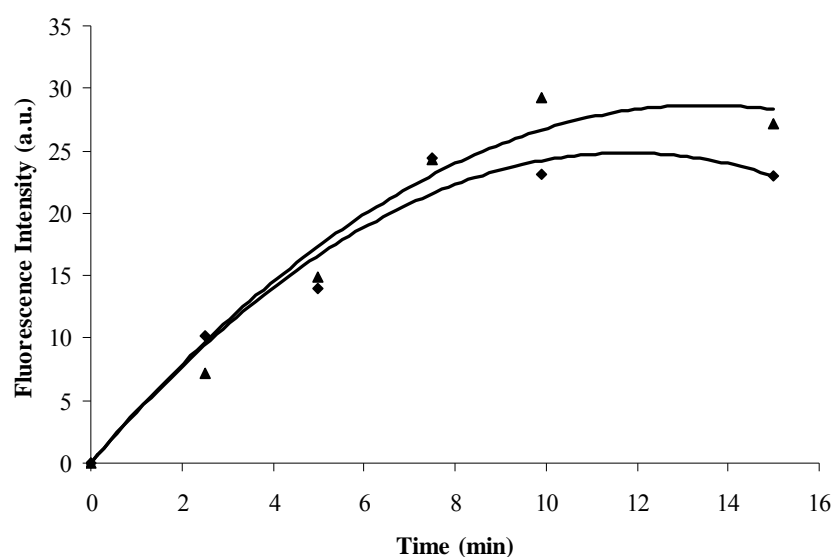


Figure 9 Time-dependent HIV-1 RT activity in the case of 30 ng/ μ l of purified HIV-1 RT (▲) and 0.5 U/ μ l commercial HIV-1 RT (◆).

In the case of nevirapine and 68NV based on time-dependent activity, the activity of both inhibitors was increased when time increased (Figure 10). But activity of HIV-1 RT was decreased when complexed with 68NV and nevirapine, respectively. From these results, it can be concluded that both 68NV and nevirapine could inhibit HIV-1 RT activity and the inhibition of 68NV was found to be higher than nevirapine.

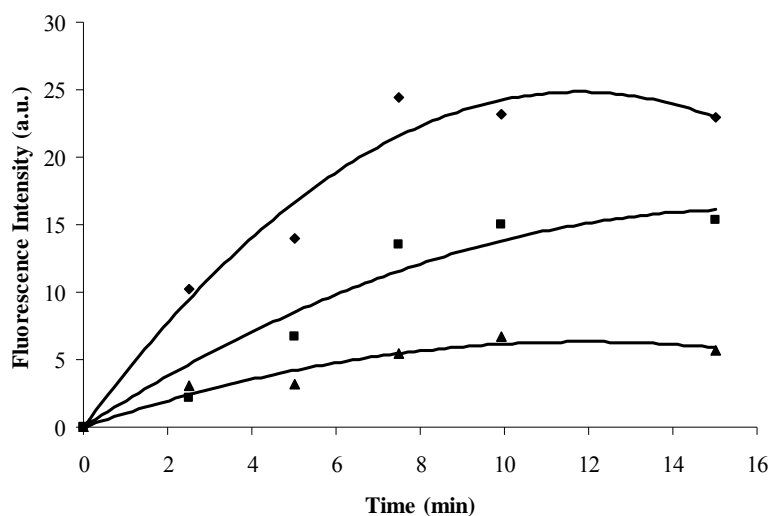


Figure 10 Time-dependent inhibition of 30 ng/μl purified HIV-1 RT activity with no inhibitor (♦), nevirapine (■) and 68NV (▲).

2. Inhibition of HIV-1 reverse transcriptase

2.1 Screening dipyrindiazepinone derivatives at 1 μM

In this work, ten of dipyrindiazepinone derivatives were used to study the inhibited efficiency of HIV-1 RT activity as shown in Table 1. The 1 μM dipyrindiazepinone derivative in each reaction was used in this experiment to study inhibition on 30 ng/μl of HIV-1 RT activity. The experiments were performed three times in order to determine average and standard deviation (mean ± S.D.). Fold relative inhibition in comparing to nevirapine was calculated by dividing the average of each dipyrindiazepinone derivative with an average of nevirapine. The results are shown in Figure 11 and Table 5. It was found that at 1 μM of NA14, NA15, NA16, NA17 and 68NV could inhibit the HIV-1 RT activity higher than nevirapine, N14, N15, N16 and NB17 with fold relative inhibition in comparing to nevirapine as 3.18, 2.42, 1.90, 2.04 and 2.55, respectively. Therefore, NA14, NA15, NA16, NA17 and 68NV were studied on the interaction of dipyrindiazepinone derivatives with HIV-1 RT compared with nevirapine. Considering standard deviation of some derivative, it was observed that standard deviations of NA15, NA16, NA17, N15 and N16 were

rather high. This might be affect from solubility of inhibitor as compared with standard deviation of nevirapine (1.793), which was lower than other derivatives.

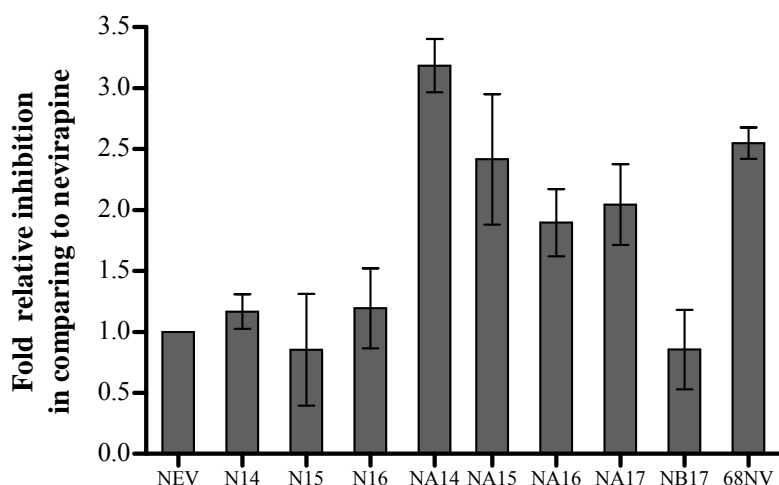


Figure 11 Fold relative inhibition in comparing to nevirapine with different dipyrroldiazepinone derivatives at 1 μ M on the purified HIV-1 RT activity.

Table 5 Percent inhibition from three independent experiments in each dipyrroldiazepinone derivative at 1 μ M. Fold relative inhibition are shown in comparison to nevirapine.

Compound	Percent inhibition	Fold relative inhibition in comparing to nevirapine
Nevirapine	31.87 \pm 1.793	1
68NV	81.17 \pm 4.717	2.55
N14	37.22 \pm 5.549	1.17
N15	26.67 \pm 12.87	0.85
N16	38.44 \pm 12.28	1.19
NA14	101.3 \pm 4.065	3.18
NA15	77.52 \pm 20.62	2.42
NA16	60.76 \pm 11.86	1.90
NA17	65.43 \pm 13.27	2.04
NB17	26.90 \pm 8.859	0.85

Furthermore, we compared percent inhibition of ten of dipyridodiazepinone derivatives at 1 μM between purified HIV-1 RT and commercial HIV-1 RT. Each experiment was repeated three times. Mean and standard deviations were determined and shown in Figure 12. Fold relative inhibition in comparing to nevirapine on purified HIV-1 RT of NA14, NA15 and 68NV differed from the commercial HIV-1 RT. It indicated that NA14, NA15 and 68NV could inhibit the purified HIV-1 RT higher than the commercial HIV-1 RT. Therefore, the activity of the commercial HIV-1 RT was higher than the activity of the purified HIV-1 RT. However, both enzymes show the same tendency. Therefore, the purified HIV-1 RT can be used in this experiment, although, the efficiency of purified HIV-1 RT is a bit lower than commercial HIV-1 RT.

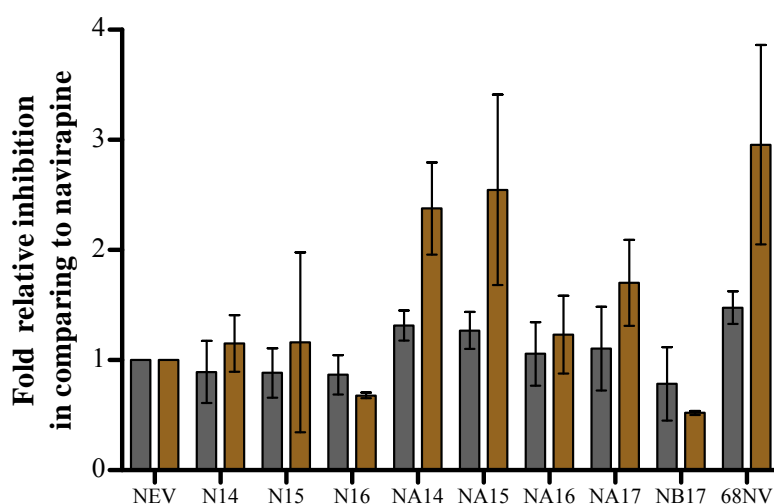


Figure 12 Fold relative inhibition in comparing to nevirapine with different dipyridodiazepinone derivatives at 1 μM on the different HIV-1 RT activity. Gray bars represent 0.5 U/ μl commercial HIV-1 RT. Brown bars represent 30 ng/ μl purified HIV-1 RT.

2.2 IC₅₀ value determination

IC₅₀ (50% inhibition concentration) is an important evidence to study the interaction of NNRTIs to HIV-1 RT. From the result of screening 1 μM dipyrindiazepinone derivatives, it was found that NA14, NA15, NA16, NA17 and 68NV could inhibit HIV-1 RT activity better than nevirapine. Therefore, NA14, NA15, NA16, NA17 and 68NV were selected to determine the IC₅₀ values. Varying concentration of each inhibitor was assayed to test against the HIV-1 RT activity. The IC₅₀ values are shown in Figure 13.

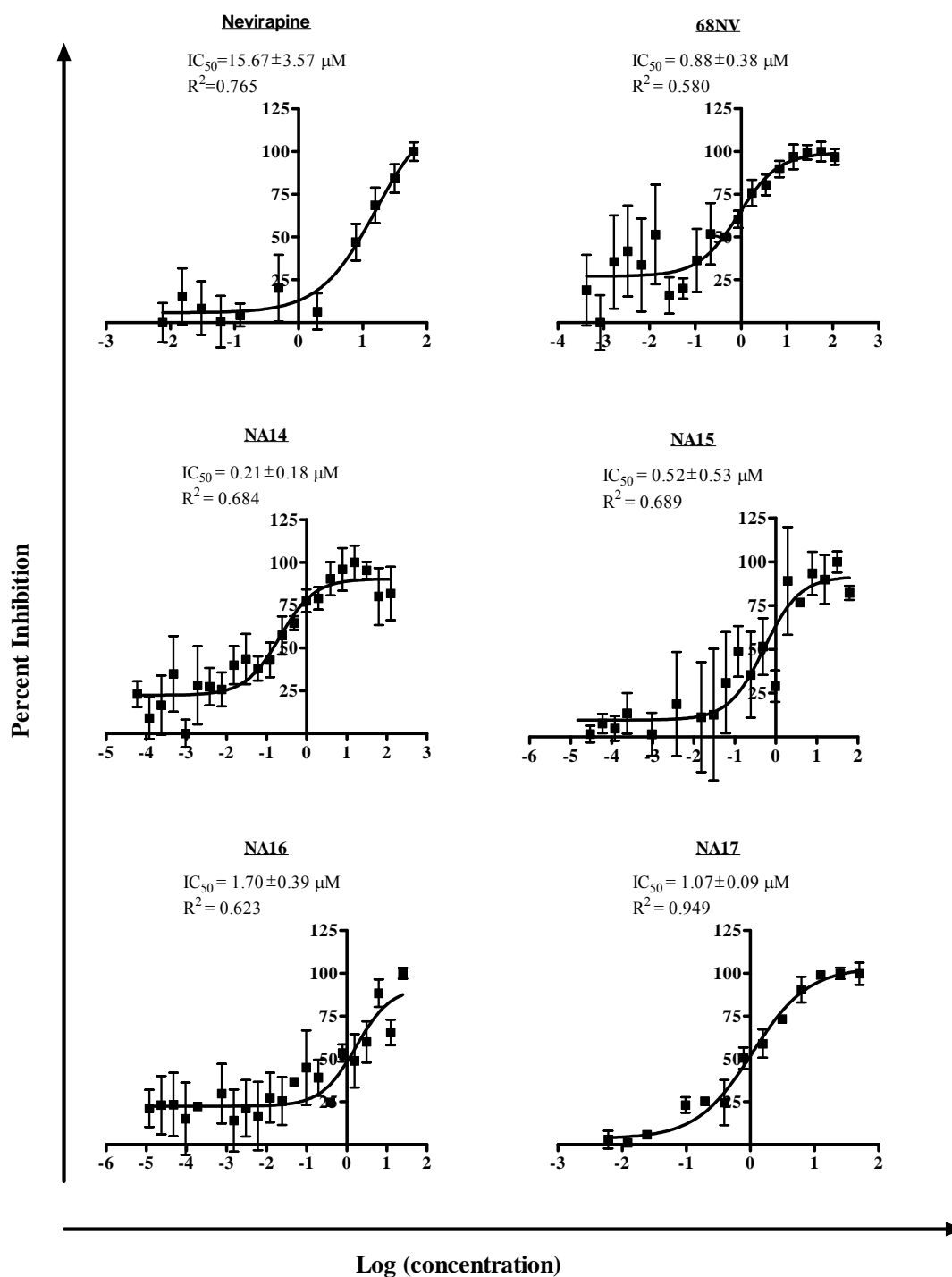


Figure 13 IC_{50} values of nevirapine, 68NV and dipyrindiazepinone derivatives on the enzymatic activities of HIV-1 RT. Dose-response curves were fitted to three-parameter logistic equation. IC_{50} and standard error are reported.

Nevirapine inhibited HIV-1 RT activity with IC_{50} value of $15.67 \pm 3.57 \mu\text{M}$ ($R^2 = 0.765$). Many works reported IC_{50} values of nevirapine such as $0.084 \mu\text{M}$ (Merluzzi *et al.*, 1990), $23 \pm 11 \mu\text{M}$ (Balzarini *et al.*, 1992), $7.22 \pm 1.38 \mu\text{M}$ (Nissley *et al.*, 2007), $2.22 \mu\text{M}$ (Hang *et al.*, 2007) and $1.7 \pm 0.2 \mu\text{M}$ (Herschhorn *et al.*, 2008). Each paper reported different IC_{50} value is found to depend on conditions and methods in each experiment. The IC_{50} value of nevirapine in the present experiment was among the range of other reports. The dipyrindiazepinone derivatives including NA14, NA15 showed to have lower IC_{50} than 68NV, NA16, NA17 and nevirapine with IC_{50} values 0.2138 and 0.5199, respectively. Therefore, inhibition HIV-1 RT activity of NA14 was found to be the highest when compared with other dipyrindiazepinone derivatives. However, the obtained curves from nevirapine and NA16, which lacked top of data point, were not able to be completed. Therefore, the obtained IC_{50} values in these two experiments might have some errors and the increasing concentration of dipyrindiazepinone derivative was required to solve this problem.

Part C: Molecular Modeling

1. Validation of docking method

Structures of the HIV-1 RT heterodimer in complexed with nevirapine and delarvidine are shown in Figure 14 and 15, respectively. The GOLD program was used for docking nevirapine and delarvidine into its binding pocket of HIV-1 RT. Comparing between GoldScore and ChemScore fitness functions, the GoldScore and ChemScore of docked nevirapine were 62.58 and 29.64, respectively. The root mean square deviation (rmsd) of docking conformation was 0.37 for GoldScore and 0.75 for ChemScore comparing to X-ray structure (PDB code 1VRT), respectively. The orientations of x-ray structure and docked nevirapine with GoldScore and ChemScore are shown in Figure 16a and 16b, respectively. The GoldScore and ChemScore of docked delarvidine were 88.16 and 43.98, respectively. The rmsds of docked delarvidine were 1.55 for GoldScore and 1.66 for ChemScore comparing to X-ray structure (PDB code 1KLM). The structural orientations of x-ray and docked delarvidine with GoldScore and ChemScore are shown in Figure 17a and 17b, respectively. Therefore, both GoldScore and ChemScore were found to reproduce the x-ray conformation both nevirapine and delarvidine.

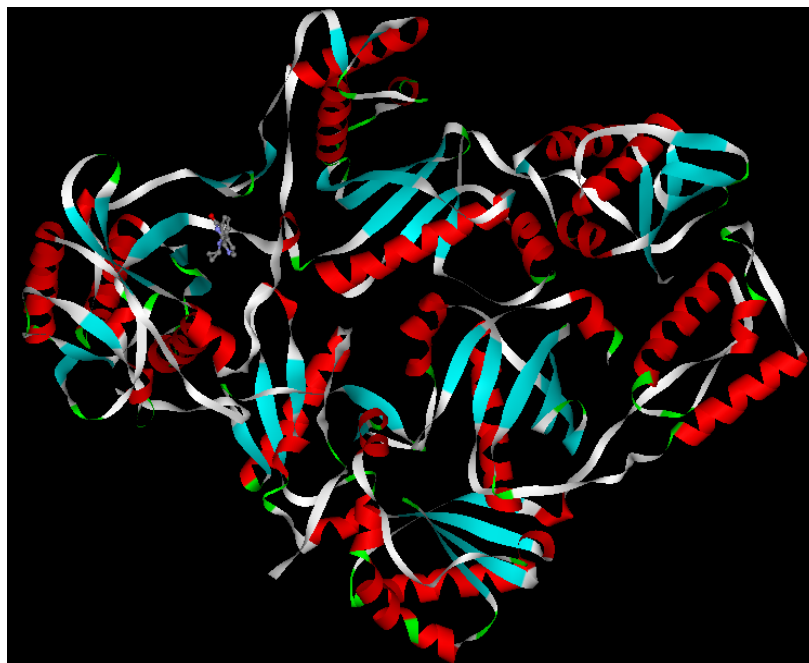


Figure 14 The structure of the HIV-1 RT heterodimer in complex with nevirapine (atom-type color) (PDB code 1VRT).

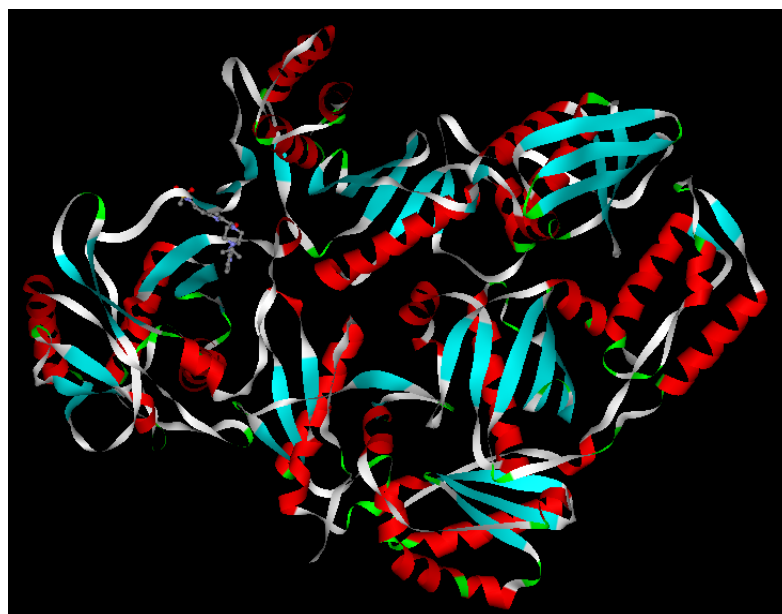
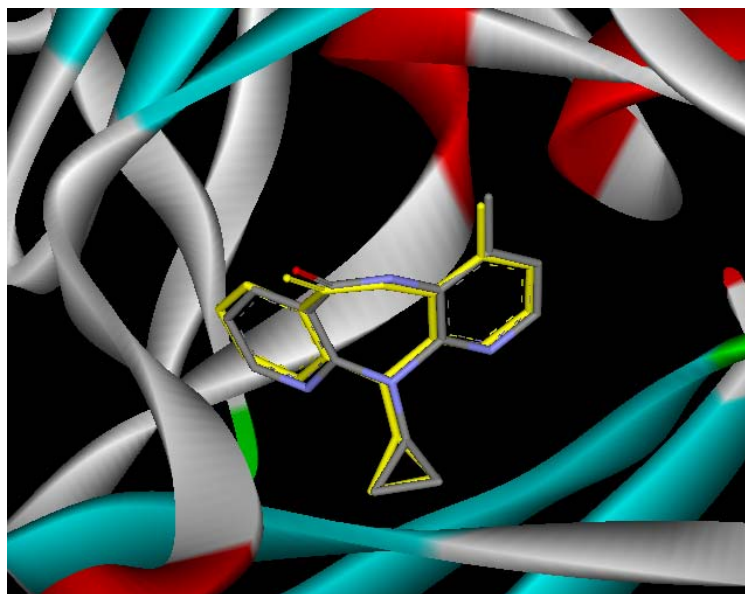
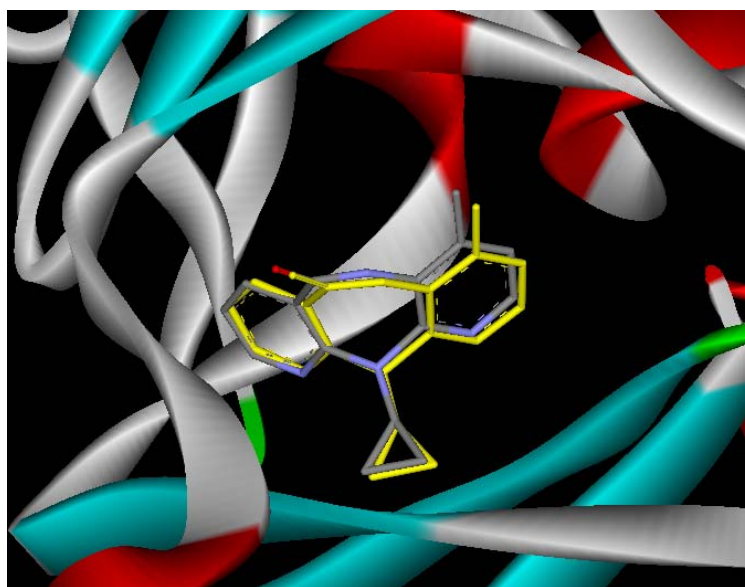


Figure 15 The structure of the HIV-1 RT heterodimer in complex with delarvidine (atom-type color) (PDB code 1KLM).

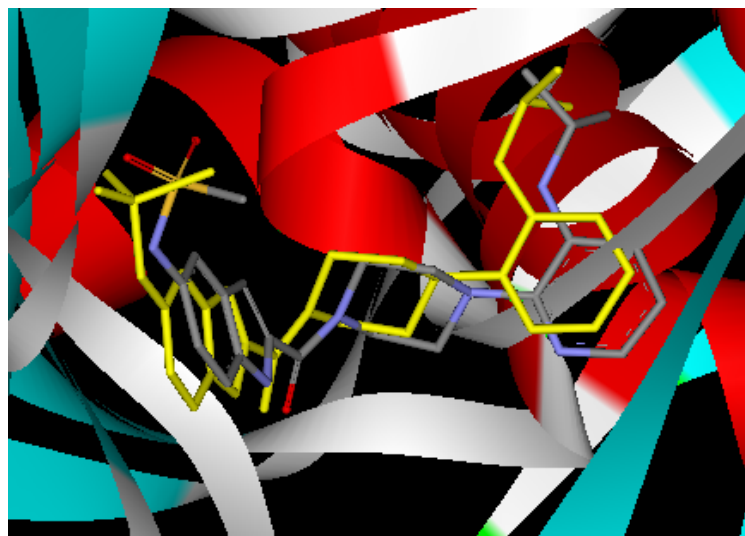


(a)

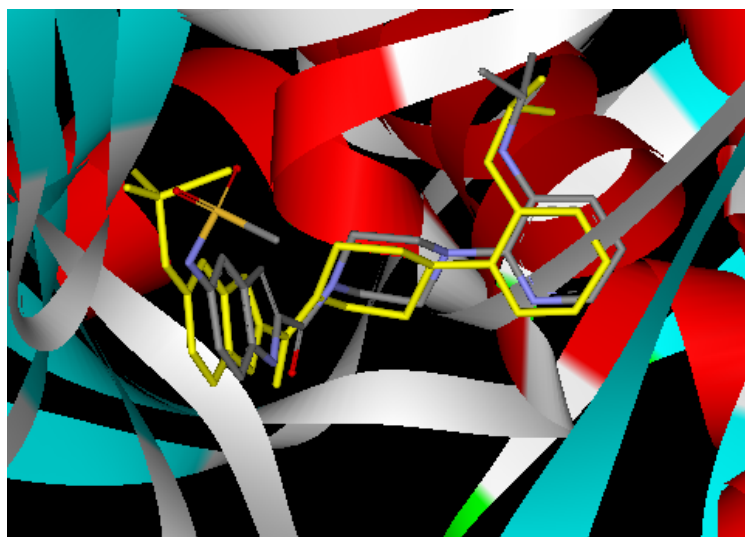


(b)

Figure 16 Orientation of nevirapine in HIV-1 RT binding pocket (PDB code 1VRT). (a) Geometries obtained from X-ray (yellow color) and docking (atom-type color) using GoldScore fitness function. (b) Geometries obtained from X-ray (yellow color) and docking (atom-type color) using the ChemScore fitness function.



(a)



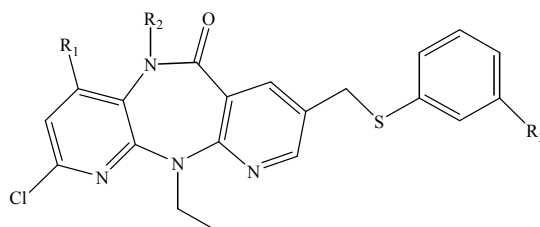
(b)

Figure 17 Orientation of delarvidine in HIV-1 RT binding pocket (PDB code 1KLM). (a) Geometries obtained from X-ray (yellow color) and docking (atom-type color) using GoldScore fitness function. (b) Geometries obtained from X-ray (yellow color) and docking (atom-type color) using the ChemScore fitness function.

2. Docking of nevirapine derivatives and 68NV derivatives

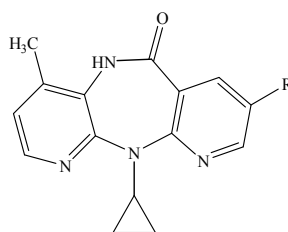
The GoldScore and ChemScore were obtained by docked N14, N15, N16, NA14, NA15, NA16 and 68NV in PDB code 1KLM of HIV-1 RT and docked NB17, NB18 and nevirapine in PDB code 1VRT of HIV-1 RT. The obtained results are shown in Table 6 and 7. The results show that the best GoldScore and ChemScore are NA16 with GoldScore of 82.58 and ChemScore of 41.77 followed by NA17, 68NV and NA15 with GoldScore of 82.28, 80.51 and 79.02, respectively and followed by NA17, 68NV, NA14 and NA15 with ChemScore of 39.58, 38.74, 38.72 and 37.96, respectively. The superimposition of 68NV derivatives in GoldScore was found that the orientations of N15, N16, NA15, NA16 and NA17 were the same as 68NV which are shown in Figure 18a. Unlike the orientations of the others, those of N14 and NA14 were different from 68NV. The orientations are shown in Figure 18b. For ChemScore, NA14, NA15, NA16 and NA17 showed the same alignment as 68NV but the orientations of N14, N15 and N16 were different as shown in Figure 19a and 19b, respectively. The structures of NB17 and NB18 were orientated in the same as nevirapine both GoldScore and ChemScore. The orientations are shown in Figure 20a and 20b.

Table 6 GoldScore and ChemScore of docked 68NV derivatives compared with 68NV in HIV-1 RT (PDB code 1KLM).

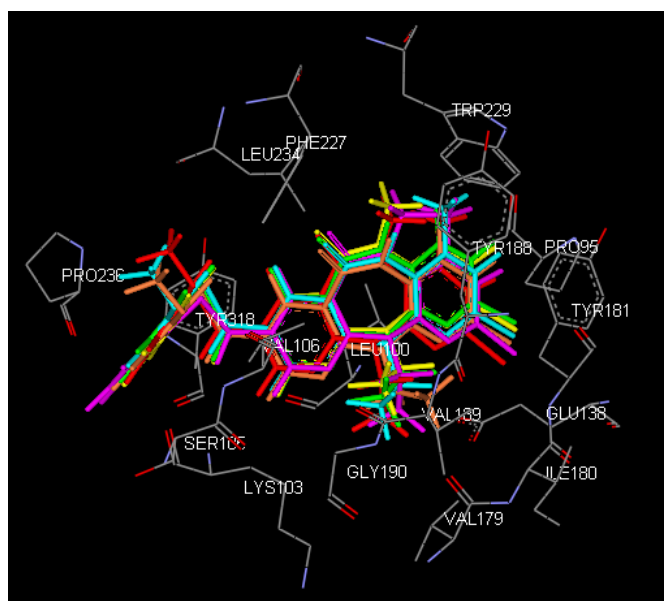


Compounds	R ₁	R ₂	R ₃	GoldScore	ChemScore
68NV	H	CH ₃	H	80.51	38.74
N14	H	H	H	62.20	32.66
N15	H	H	OCH ₃	72.24	34.06
N16	H	H	F	72.83	32.58
NA14	CH ₃	H	H	66.07	38.72
NA15	CH ₃	H	OCH ₃	79.02	37.96
NA16	CH ₃	CH ₃	OCH ₃	82.58	41.77
NA17	CH ₃	CH ₃	H	82.28	39.58

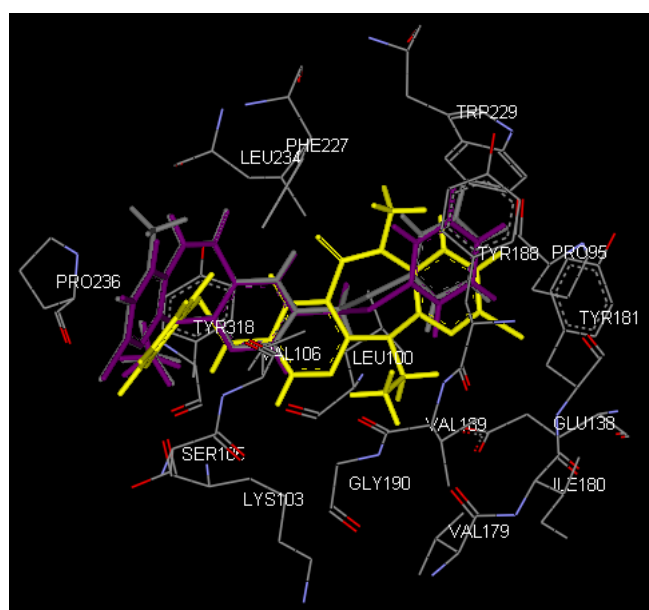
Table 7 GoldScore and ChemScore of docked nevirapine derivatives and nevirapine in HIV-1 RT (PDB code 1VRT).



Compounds	R	GoldScore	ChemScore
Nevirapine	H	62.58	29.64
NB17	NH ₃ ⁺	71.24	31.42
NB18	NH ₂	67.09	33.01

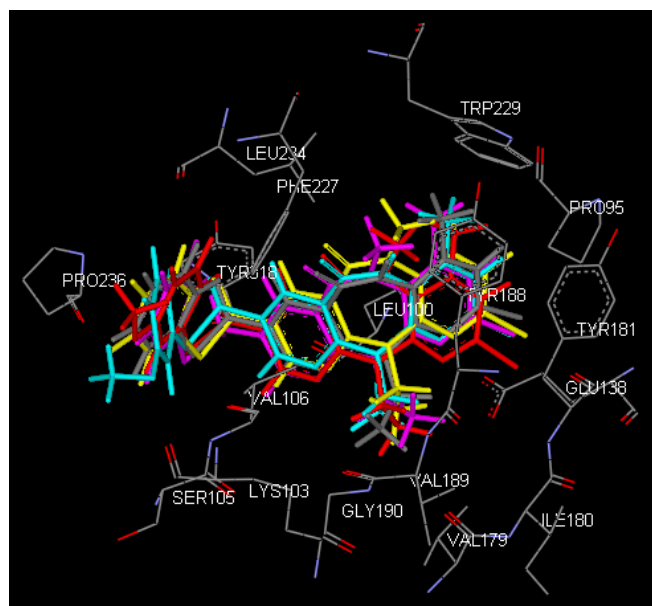


(a)

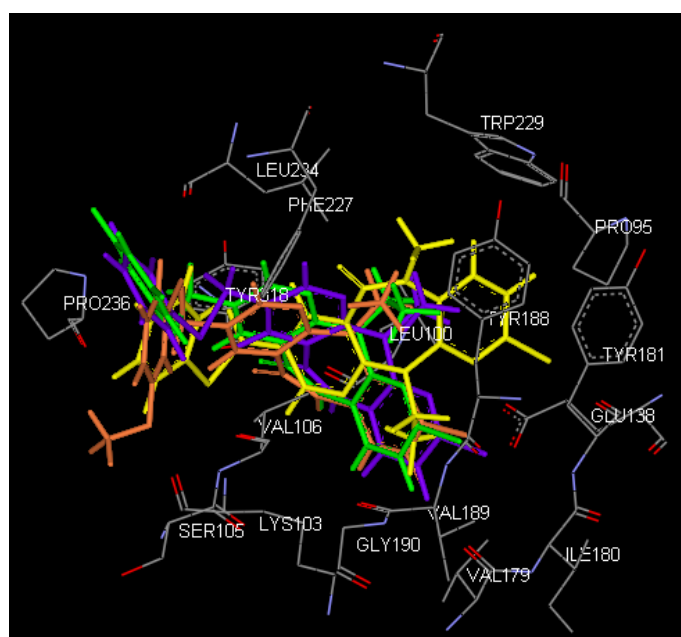


(b)

Figure 18 Superimpositions of 68NV (yellow) compared with (a) orientations of N15 (orange), N16 (green), NA15 (blue), NA16 (red) and NA17 (pink) and (b) orientations of N14 (purple) and NA14 (gray) using the GoldScore fitness function.

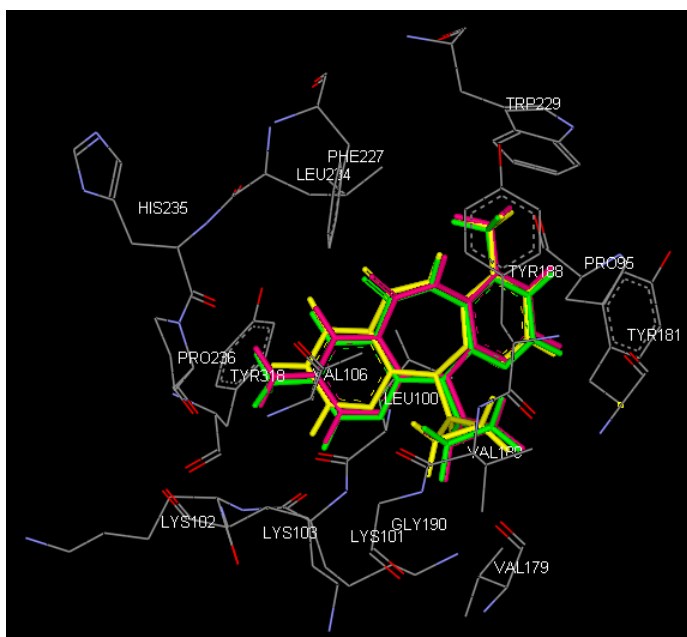


(a)

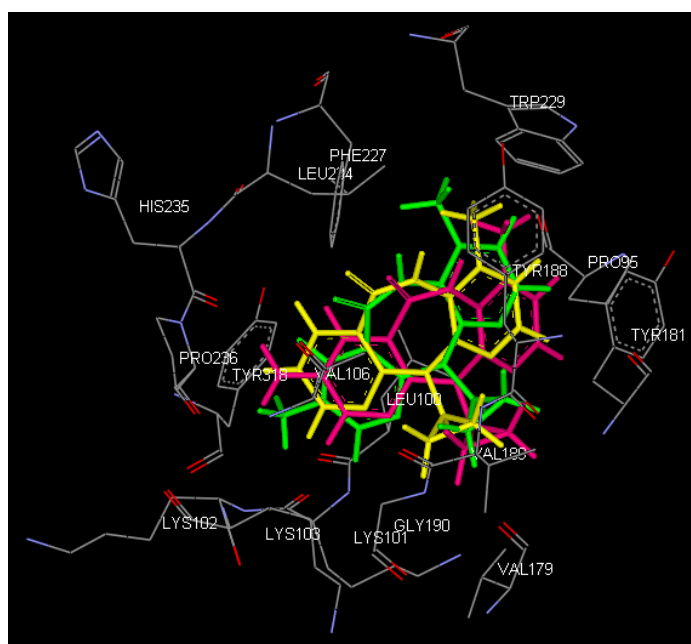


(b)

Figure 19 Superimpositions of 68NV (yellow) compared with (a) orientations of N15 (orange), N16 (green), NA15 (blue), NA16 (red) and NA17 (pink) and (b) orientations of N14 (purple) and NA14 (gray) using the ChemScore fitness function.



(a)



(b)

Figure 20 Superimpositions of nevirapine (yellow) compared with orientations of NB17 (green) and NB18 (pink) using (a) GoldScore and (b) ChemScore fitness function.

From orientation of each compound, ChemScore was chosen to study the interaction due to the docked orientations of NA14, NA15, NA16 and NA17. These results were the same results as screening dipyridodiazepinone derivatives at 1 μM because fold relative inhibition in comparing to nevirapine of NA14, NA15, NA16 and NA17 closed to 68NV and these compounds could inhibit the HIV-1 RT activity higher than nevirapine. The orientations are shown in Figure 19a. The thiophenyl side chain interacts with some residues such as Lys103, Val106, Phe227, Leu234, His235, Pro236 and Tyr318. The present of methyl group at R₂ position of 68NV reproduced a good binding interaction to Tyr188. Additionally, the methyl group at R₁ position of NA14 and NA15 have affected to the diazepinone ring move upwards comparing to 68NV. Furthermore, the methyl group at R₁ interacts with Trp229. The methoxy group at thiophenyl side chain of NA15 generates the H-bonding with backbone of residue Val106 with 2.86 Å. Docked orientations of NA16 and NA17 showed that the presents of methyl groups at R₁ and R₂ interacts with Trp229 and Tyr188, respectively. Furthermore, the methoxy group of NA16 at the thiophenyl side chain revealed the interaction to Phe227. However, the rotatable bond of methoxy group of NA15 and NA16 is the key point for obtaining the different interaction.

For NB17, the $-\text{NH}_3^+$ group at R₁ position presents H-bonding with backbone of Lys101 and Pro236 as 1.89 and 1.96 Å, respectively. As the result, the structure of NB17 shifted to the right side of binding pocket when compared with nevirapine. For NB18, the $-\text{NH}_2$ group at R₁ generated the H-bonding with backbone of His235 and Pro236 with 1.95 and 2.10 Å, respectively. It is indicated that the structure of NB18 shifted down when compared with nevirapine. Therefore, NB17 and NB18 are considered to be good inhibitors for binding interaction to the HIV-1 RT binding pocket compared with nevirapine due to these interactions.

Comparing between the docking with ChemScore fitness function and the experimental data, the IC₅₀ values of NA14, NA15, NA16 and NA17 are close to 68NV because of the interaction of thiophenyl side chain with some residues. The presents of methyl groups at R₁ and R₂ interact with Tyr188 and Trp229, respectively.

Moreover, the methoxy groups of NA15 and NA16 could generate interaction with Val106 and Phe227, respectively. But N14, N15 and N16 showed less potential in inhibition than 68NV, NA14, NA15, NA16 and NA17. Because the lacks the methyl groups at R₁ and R₂ of N14, N15 and N16 might loss some interaction in HIV-1 RT binding pocket. Therefore, the orientations of N14, N15 and N16 differed from 68NV.

CONCLUSION

In this work, HIV-1 RT was expressed and purified by bacteria containing recombinant plasmids of p51 and p66. The concentration of HIV-1 RT in each purification step was determined by Bradford method. The purified HIV-1 RT was 14.06 mg from 1 liter of cell culture and had a purification fold of 106. The fluorometric assay could be used to determine HIV-1 RT activity in each purification step. Increasing of specific activity and fold purification were observed from cell lysate, protein precipitation, phosphocellulose P11 column and DEAE cellulose, respectively.

The purified HIV-1 RT was compared efficiency with commercial HIV-1 RT. The 30 ng/ μ l purified HIV-1 RT was equivalent to 0.5 U/ μ l commercial HIV-1 RT. The activity of 0.5 U/ μ l commercial HIV-1 RT was a slightly better than 30 ng/ μ l purified HIV-1 RT. Therefore, the purified HIV-1 RT could be used to study the inhibition of HIV-1 RT activity. From screening ten of dipyrindiazepinone derivatives at 1 μ M to determine percent inhibition by comparing to nevirapine, the results showed that the purified HIV-1 RT could be used in this experiment. Although, the purified HIV-1 RT showed less activity than the commercial HIV-1 RT, however, it showed the same tendency.

From screening of ten of dipyrindiazepinone derivatives, inhibitions of the purified HIV-1 RT activities with NA14, NA15, NA16, NA17 and 68NV were found to be greater than nevirapine with fold relative inhibition as 3.18, 2.42, 1.90, 2.04 and 2.55, respectively. These dipyrindiazepinone derivatives were selected to determine IC_{50} value in comparison with nevirapine to study interaction of dipyrindiazepinone derivatives with HIV-1 RT. The results showed that nevirapine could inhibit the HIV-1 RT activity with IC_{50} values 15.67 μ M, while IC_{50} values of NA14 and NA15 were 0.2138 and 0.5199 μ M, respectively, which higher than nevirapine (fold IC_{50} values as 73.29 and 30.14, respectively). The obtained results indicated that NA14 was the best inhibitor among other dipyrindiazepinone derivatives in this study.

According to molecular docking by using GOLD program, the docking with ChemScore fitness function was selected to consider the interaction of dipyrrodothiazepinone derivatives in the HIV-1 RT binding pocket. Based on the docking calculations, more understanding of the orientation of the bound inhibitors, the highest inhibitions, NA14 and NA15, were analyzed. Their thiophenyl side chain could interact with some residues such as Lys103, Val106, Phe227, Leu234, His235, Pro236 and Tyr318. The present of methyl group at R₁ position can interact with Trp229. Furthermore, the methoxy group at thiophenyl side chain of NA15 could generate the H-bonding with backbone of residue Val106 with 2.86 Å.

Taken into account, the kinetic investigation of HIV-1 RT and NNRTI were successfully developed based on fluorescence bioassay and will be used further screening for new biological active compounds for anti-HIV drug.

LITERATURE CITED

- Ahn, S.J., J. Costa and J.R. Emanuel. 1996. PicoGreen quantitation of DNA: effective evaluation of samples pre- or post-PCR. **Nucleic Acids Res.** 24: 2623-5.
- Balzarini, J., M.J. Perez-Perez, A. San-Felix, M.J. Camarasa, I.C. Bathurst, P.J. Barr and E. De Clercq. 1992. Kinetics of inhibition of human immunodeficiency virus type 1 (HIV-1) reverse transcriptase by the novel HIV-1-specific nucleoside analogue [2',5'-bis-O-(tert-butyldimethylsilyl)-beta-D-ribofuranosyl]-3'-spiro-5''-(4''-amino-1'',2''-oxathiole-2'',2''-dioxide)thymine (TSAO-T). **J. Biol. Chem.** 267(17): 11831-11838.
- Barreca M.L., A. Rao, L.D. Luca, M. Zappala, A.M. Monforte, G. Maga, C. Pannecouque, J. Balzarini, E. De Clercq, A. Chimirri and P. Monforte. 2005. Computational strategies in discovering novel non-nucleoside inhibitors of HIV-1 RT. **J. Med. Chem.** 48: 3433-3437.
- Busschots, K., J.D. Rijck, F. Christ and Z. Debyser. 2009. Insearch of small molecules blocking interaction between HIV proteins and intracellular cofactors. **Mol. Biosyst.** 5: 21-31.
- Chavan, S.J. and H.J. Prochaska. 1995. Fluorometric measurement of reverse transcriptase activity with 4',6-Diamidino-2-phenylindole. **Anal. Biochem.** 225: 54-59.
- Cosa, G., K.S. Focsaneanu, J.R.N. McLean, J.P. McNamee and J.C. Scaiano. 2001. Photophysical properties of fluorescent DNA-dyes bound to single- and double-stranded DNA in aqueous buffered solution. **Photochem. Photobiol.** 73: 585-599.

- Das, K., J.D. Bauman, A.D. Clark, Jr., Y.V. Frenkel, P.J. Lewi, A.J. Shatkin, S.H. Hughes and E. Arnold. 2008. High-resolution structures of HIV-1 reverse transcriptase/TMC278 complexes: Strategic flexibility explains potency against resistance mutations. **Proc. Nat. Acad. Sci. U.S.A.** 105(5): 1466-1471.
- Das, K., P.J. Lewi, S.H. Hughes and E. Arnold. 2005. Crystallography and the design of anti-AIDS drugs: conformational flexibility and positional adaptability are important in the design of non-nucleoside HIV-1 reverse transcriptase inhibitors. **Prog. Biophys. Mol. Biol.** 88: 209–231.
- De Clercq E. 1997. Development of resistance of human immunodeficiency virus (HIV) to anti-HIV agents: how to prevent the problem? **Int. J. Antimicrob. Agents.** 9: 21-26.
- De Jonge M.R., L.M.H. Koymans, H.M. Vinkers, F.F.D. Daeyaert, J. Heeres, P.J. Lewi and P.A.J. Janssen. 2005. Structure Based Activity Prediction of HIV-1 Reverse Transcriptase Inhibitors. **J. Med. Chem.** 48: 2176-2183.
- Debnath, A.K. 2005. Application of 3D-QSAR Techniques in Anti-HIV-1 Drug Design – An Overview. **Curr. Pharm. Des.** 11: 3091-3110.
- Divita, G., B. Muller, U. Immendorfer, M. Gaute1, K. Rittinger, T. Restle and R.S. Goody. 1993. Kinetics of Interaction of HIV Reverse Transcriptase with Primer/Template. **Biochemistry.** 32: 7966-7971.
- Geitmann, M., T. Unge and U.H. Danielson. 2006. Interaction Kinetic Characterization of HIV-1 Reverse Transcriptase Non-nucleoside Inhibitor Resistance. **J. Med. Chem.** 49: 2375-2387.

- Geitmann, M., T. Unge and U.H. Danielson. 2006. Biosensor-Based Kinetic Characterization of the Interaction between HIV-1 Reverse Transcriptase and Non-nucleoside Inhibitors. **J. Med. Chem.** 49: 2367-2374.
- Hang J.Q., Y. Li, Y. Yang, N. Cammack, T. Mirzadegan and K. Klumpp. 2007. Substrate-dependent inhibition or stimulation of HIV RNase H activity by non-nucleoside reverse transcriptase inhibitors (NNRTIs). **Biochem. Biophys. Res. Commun.** 352: 341–350.
- Hannongbua, S. 2006. Structural Information and Drug-Enzyme Interaction of the Non-Nucleoside Reverse Transcriptase Inhibitors Based on Computational Chemistry Approaches. **Top Heterocycl Chem.** 4: 55-84.
- Herschhorn, A. and A. Hizi. 2008. Virtual Screening, Identification, and Biochemical Characterization of Novel Inhibitors of the Reverse Transcriptase of Human Immunodeficiency Virus Type-1. **J. Med. Chem.** 51: 5702-5713.
- _____, I. Oz-Gleenberg and A. Hizi. 2008. Mechanism of Inhibition of HIV-1 Reverse Transcriptase by the Novel Broad-Range DNA polymerase Inhibitor N-are-2-(2-thienyl)acetamide. **Biochemistry.** 47: 490-502.
- Ihmels H. and D. Otto. 2005. Intercalation of Organic Dye Molecules into Double-Stranded DNA General Principles and Recent Developments. **Top. Curr. Chem.** 258: 161-204.
- Jacobo-Molina, A., J. Ding, R.G. Nanni, A.D. Clark, Jr., X. Lu, C. Tantillo, R.L. Williams, G. Kamer, A.L. Ferris, P. Clark, A. Hizi, S.H. Hughes and E. Arnold. 1993. Crystal structure of human immunodeficiency virus type 1 reverse transcriptase complexed with double-stranded DNA at 3.0 Å resolution shows bent DNA. **Proc. Nat. Acad. Sci. U.S.A.** 90: 6320-6324.

- Jonckheere, H., J. Anne and E. De Clercq. 2000. The HIV-1 reverse transcription Process as Target for RT Inhibitors. **Med Res Rev** 20(2): 129-154.
- Karlsen, F., H.B. Steen and J.M. Nesland. 1995. SYBR green I DNA staining increases the detection sensitivity of viruses by polymerase chain reaction. **J Virol Methods**. 55: 153-6.
- Khunnawutmanotham, N., N. Chimnoi, P. Saparpakorn, P. Pungpo, S. Louisirirochanakul, S. Hannongbua and S. Techasakul. 2007. Novel 2-Chloro-8-arylthiomethyl diazepinone Derivatives with Activity against HIV-1 Reverse Transcriptase. **Molecules**. 12: 218-230.
- Kuno, M., S. Hannongbua and K. Morokuma. 2003. Theoretical investigation on nevirapine and HIV-1 RT binding site interaction, based on ONIOM method. **Chem. Phys. Lett.** 380: 456-463.
- Merluzzi, V.J., K.D. Hargrave, M. Labadia, K. Grozinger, M. Skoog, J.C. Wu, C.K. Shih, K. Eckner, S. Hattox, J. Adams, A.S. Rosethal, R. Faanes, R.J. Eckner, R.A. Koup and J.L. Sullivan. 1990. Inhibition Of HIV-1 Replication by a Nonnucleoside Reverse Transcriptase Inhibitor. **Science** 250: 1411-1413.
- Nissley, D.V., J. Radzio, Z. Ambrose, C.W. Sheen, N. Hamamouch, K.L. Moore, G. Tachedjian and N. Sluis-Cremer. 2007. Characterization of novel non-nucleoside reverse transcriptase (RT) inhibitor resistance mutations at residues 132 and 135 in the 51 kDa subunit of HIV-1 RT. **Biochem. J** 404: 151-157.
- Pungpo, P., S. Saparpakorn, P. Wolschann and S. Hannongbua. 2006. Computer-aided molecular design of highly potent HIV-1 RT inhibitors: 3D QSAR and molecular docking studies of efavirenz derivatives. **SAR QSAR Environ Res** 17(4): 353-370.

- Ren, J., R. Esnouf, E. Garman, D. Somers, C. Ross, I. Kirby, J. Keeling, G. Darby, Y. Jone, D. Stuart and D. Stammers. 1995. High resolution structure of HIV-1 RT from four RT – inhibition complex. **Nature Struct Biol** 2(4): 293-302.
- Ren, J. and D.K. Stammers. 2008. Structure basis for drug resistance mechanisms for non-nucleoside inhibitors of HIV reverse transcriptase. **Virus Res** 134: 157-170.
- Rengarajan, K., S.M. Cristol, M. Mehta and J.M. Nickerson. 2002. Quantifying DNA concentrations using fluorometry: A comparison of fluorophores. **Mol Vis** 8: 416-21.
- Rye, H.S., S. Yue, M.A. Quesada, R.P. Haugland, R.A. Mathies and A.N. Glazer. 1993. Picogram detection of stable dye-DNA intercalation complexes with two-color laser-excited confocal fluorescence gel scanner. **Methods Enzymol.** 217: 414-31.
- Saparpakorn, S., S. Hannongbua and D. Rognan. 2006. Design of nevirapine derivatives insensitive to the K103N and Y181C HIV-1 reverse transcriptase mutants. **SAR QSAR Environ Res** 17(2): 183-194.
- Sarafianos, S.G., K. Das, C. Tantillo, A.D. Clark Jr, J. Ding, J.M. Whitcomb, P.L. Boyer, S.H. Hughes and E. Arnold. 2001. Crystal structure of HIV-1 reverse transcriptase in complex with a polypurine tract RNA:DNA. **EMBO J.** 20(6): 1449-1461.
- Seville, M., A.B. West, M.G. Cull and C.S. McHenry. 1996. Fluorometric assay for DNA polymerases and reverse transcriptase. **BioTechniques** 21: 664-672.
- Singer, V.L., L.J. Jones, S.T. Yue and R.P. Haugland. 1997. Characterization of PicoGreen Reagent and Development of a Fluorescence-Based Solution Assay for Double-Stranded DNA Quantitation. **Anal. Biochem.** 249: 228-238.

Sluis-Cremer, N. and G. Tachedjian. 2008. Mechanisms of inhibition of HIV replication by non-nucleoside reverse transcriptase inhibitors. **Virus Res** 134: 147-156.

APPENDICES

APPENDIX A

IC₅₀ determination from fluorometric assay

IC₅₀ determination from fluorometric assay

IC₅₀ is determined using fluorometric method. The concentration of NNRTIs was varied by two-fold serial dilution. The activity of HIV-1 RT was detected by PicoGreen reagent after dTTP incorporated into poly(A) ribonucleotide template and oligo d(T)₁₆ primer generated the RNA-DNA heteroduplexes, increasing the fluorescence intensity (Victoria, 1997). The products of RNA-DNA heteroduplexes in each concentration of NNRTI were calculated as percent inhibition by comparing to in the case of no inhibitor. IC₅₀ can be determined from plotting between the logarithm of agonist concentration and percent inhibition. Nonlinear regression curves were fitted to three-parameter logistic equation. The raw data and the result from curves fitting of nevirapine, 68NV, NA14, NA15, NA16 and NA17 were reported.

1. Nevirapine

Appendix Table A1 Fluorescence intensity and percent inhibition in each concentration of nevirapine.

Concentration (μM)	Log (conc.)	Fluorescence Intensity			Percent Inhibition		
		1	2	3	1	2	3
62.50	1.796	51.65	48.97	47.24	49.82	53.06	47.43
31.25	1.495	52.51	50.63	49.29	47.48	48.30	40.55
15.63	1.194	53.15	53.01	50.89	45.74	41.47	35.17
7.81	0.893	56.37	54.16	52.99	36.97	38.17	28.12
1.95	0.291	60.29	58.86	56.55	26.29	24.69	16.16
0.49	-0.311	60.10	54.82	56.53	26.80	36.28	16.23
0.12	-0.913	62.33	58.54	55.72	20.73	25.61	18.95
0.06	-1.214	61.03	58.44	57.88	24.27	25.90	11.70
0.03	-1.515	58.72	59.20	57.04	30.56	23.72	14.52
0.02	-1.816	59.09	56.93	56.85	29.56	30.23	15.16
0.01	-2.118	60.45	60.02	57.16	25.85	21.37	14.12
No inhibitor	-	69.94	67.47	61.36	-	-	-

Appendix Table A2 Values from calculation of nevirapine using Nonlinear regression curves to fit to three-parameter logistic equation.

Dose-response curve	Values
Best-fit values	
BOTTOM	5.778
TOP	124.7
LOGIC ₅₀	1.195
IC ₅₀	15.67
Std. Error	
BOTTOM	4.69
TOP	23.08
LOGIC ₅₀	0.2404
95% Confidence Intervals	
BOTTOM	-3.798 - 15.35
TOP	77.62 - 171.9
LOGIC ₅₀	0.7042 - 1.686
IC ₅₀	5.060 - 48.50
Goodness of Fit	
Degrees of Freedom	30
R ²	0.7658
Absolute Sum of Squares	11804
Sy.x	19.84
Data	
Number of X values	14
Number of Y replicates	3
Total number of values	33
Number of missing values	9

2. 68NV

Appendix Table A3 Fluorescence intensity and percent inhibition in each concentration of 68NV.

Concentration (μM)	Log (conc.)	Fluorescence Intensity			Percent Inhibition		
		1	2	3	1	2	3
110.0000	2.041	39.53	37.81	37.84	75.02	86.53	84.79
55.0000	1.740	39.17	36.06	36.97	75.84	91.06	86.91
27.5000	1.439	38.39	37.78	36.3	77.60	86.61	88.53
13.7500	1.138	40.32	40.18	34.56	73.24	80.41	92.77
6.8750	0.837	41.23	42.48	38.23	71.18	74.46	83.84
3.4375	0.536	45.09	45.65	40.4	62.46	66.26	78.56
1.7188	0.235	49.1	43.4	43.58	53.40	72.08	70.83
0.8594	-0.066	51.74	51.51	47.67	47.44	51.10	60.88
0.4297	-0.367	53.45	53.05	54.58	43.58	47.12	44.07
0.2148	-0.668	61.53	42.78	56.17	25.32	73.68	40.20
0.1074	-0.969	70.08	49.73	56.09	6.01	55.71	40.40
0.0537	-1.270	67.63	61.8	61.62	11.54	24.49	26.94
0.0269	-1.571	71.74	59.09	64.65	2.26	31.50	19.57
0.0134	-1.872	69.09	37.19	55.48	8.25	88.14	41.88
0.0067	-2.173	75.7	44.92	58.61	-6.69	68.15	34.27
0.0034	-2.474	72.29	42.63	56.29	1.02	74.07	39.91
0.0017	-2.775	74.69	43.96	58.79	-4.40	70.63	33.83
0.0008	-3.076	81.68	63.74	66.1	-20.19	19.47	16.05
0.0004	-3.377	77.74	54.22	61.26	-11.29	44.09	27.82
No inhibitor	-	72.74	71.27	72.70	-	-	-

Appendix Table A4 Values from calculation of 68NV using Nonlinear regression curves to fit to three-parameter logistic equation.

Dose-response curve	Values
Best-fit values	
BOTTOM	27.13
TOP	99.37
LOGIC ₅₀	-0.05777
IC ₅₀	0.8754
Std. Error	
BOTTOM	5.278
TOP	7.495
LOGIC ₅₀	0.2506
95% Confidence Intervals	
BOTTOM	16.54 - 37.72
TOP	84.34 - 114.4
LOGIC ₅₀	-0.5605 - 0.4450
IC ₅₀	0.2751 - 2.786
Goodness of Fit	
Degrees of Freedom	54
R ²	0.5798
Absolute Sum of Squares	35191
Sy.x	25.53
Data	
Number of X values	19
Number of Y replicates	3
Total number of values	57
Number of missing values	0

3. NA14

Appendix Table A5 Fluorescence intensity and percent inhibition in each concentration of NA14.

Concentration (μM)	Log (conc.)	Fluorescence Intensity			Percent Inhibition		
		1	2	3	1	2	3
125.00000	2.097	51.19	35.56	41.2	69.84	93.10	70.92
62.50000	1.796	42.58	37.49	44.33	81.27	88.60	61.46
31.25000	1.495	43.01	37.31	36.98	80.70	89.02	83.69
15.62500	1.194	44.75	34.66	36.01	78.39	95.20	86.62
7.81250	0.893	48.91	35.79	35.27	72.87	92.57	88.86
3.90625	0.592	49.06	38.57	35.69	72.67	86.09	87.59
1.95313	0.291	50.76	41.98	37.83	70.41	78.13	81.12
0.97656	-0.010	46.23	45.47	37.84	76.43	69.99	81.09
0.48828	-0.311	54.4	44.83	41	65.58	71.49	71.53
0.24414	-0.612	58.02	49.55	39.25	60.78	60.48	76.82
0.12207	-0.913	59.49	53.77	42.28	58.82	50.64	67.66
0.06104	-1.214	63.72	52.68	43.66	53.21	53.18	63.48
0.03052	-1.515	57.87	55.67	41.24	60.97	46.21	70.80
0.01526	-1.816	68.17	49.82	42.95	47.30	59.85	65.63
0.00763	-2.118	70.96	54.68	44.85	43.60	48.52	59.89
0.00381	-2.419	68.58	55.93	44.16	46.76	45.60	61.97
0.00191	-2.720	69.42	59.86	40.37	45.64	36.44	73.43
0.00095	-3.021	70.24	58.83	54.41	44.55	38.84	30.97
0.00048	-3.322	51.31	60.83	44.34	69.68	34.17	61.43
0.00024	-3.623	60.3	62.74	47.73	57.75	29.72	51.17
0.00012	-3.924	74.28	60.77	46.75	39.19	34.31	54.14
0.00006	-4.225	68.39	56.44	45.96	47.01	44.41	56.53
No inhibitor	-	103.8	75.48	64.65	-	-	-

Appendix Table A6 Values from calculation of NA14 using Nonlinear regression curves to fit to three-parameter logistic equation.

Dose-response curve	Values
Best-fit values	
BOTTOM	22.41
TOP	90.44
LOGIC ₅₀	-0.67
IC ₅₀	0.2138
Std. Error	
BOTTOM	3.966
TOP	4.733
LOGIC ₅₀	0.1956
95% Confidence Intervals	
BOTTOM	14.48 - 30.34
TOP	80.98 - 99.90
LOGIC ₅₀	-1.061 - -0.2790
IC ₅₀	0.08689 - 0.5260
Goodness of Fit	
Degrees of Freedom	63
R ²	0.6835
Absolute Sum of Squares	25600
Sy.x	20.16
Data	
Number of X values	22
Number of Y replicates	3
Total number of values	66
Number of missing values	0

4. NA15

Appendix Table A7 Fluorescence intensity and percent inhibition in each concentration of NA15.

Concentration (μM)	Log (conc.)	Fluorescence Intensity		Percent Inhibition	
		1	2	1	2
62.50000	1.796	43.3	43.76	74.89	70.03
31.25000	1.495	40.55	37.53	79.55	86.76
15.62500	1.194	46.96	38	68.70	85.50
7.81250	0.893	45.21	37.54	71.66	86.74
3.90625	0.592	47.28	43.71	68.15	70.16
1.95313	0.291	53.3	34.37	57.96	95.25
0.97656	-0.010	67.02	52.81	34.73	45.72
0.48828	-0.311	61.5	46.12	44.08	63.69
0.24414	-0.612	70.23	47.87	29.29	58.99
0.12207	-0.913	51.5	53.63	61.01	43.51
0.06104	-1.214	73.41	47.9	23.91	58.91
0.03052	-1.515	83.09	50.06	7.52	53.10
0.01526	-1.816	81.35	51.77	10.46	48.51
0.00381	-2.419	78.13	50.46	15.92	52.03
0.00095	-3.021	78.03	58.28	16.09	31.02
0.00024	-3.623	65.19	60.95	37.83	23.85
0.00012	-3.924	74.96	58.7	21.28	29.89
0.00006	-4.225	73.38	58.45	23.96	30.56
0.00003	-4.526	75.29	59.95	20.73	26.53
0.00001	-4.827	78.06	58.93	16.04	29.27
No inhibitor	-	87.53	69.83	-	-

Appendix Table A8 Values from calculation of NA15 using Nonlinear regression curves to fit to three-parameter logistic equation.

Dose-response curve	Values
Best-fit values	
BOTTOM	28.49
TOP	78.11
LOGIC ₅₀	-0.2841
IC ₅₀	0.5199
Std. Error	
BOTTOM	3.289
TOP	5.048
LOGIC ₅₀	0.2406
95% Confidence Intervals	
BOTTOM	21.82 - 35.16
TOP	67.87 - 88.34
LOGIC ₅₀	-0.7719 - 0.2037
IC ₅₀	0.1691 - 1.599
Goodness of Fit	
Degrees of Freedom	37
R ²	0.689
Absolute Sum of Squares	7212
Sy.x	13.96
Data	
Number of X values	23
Number of Y replicates	2
Total number of values	40
Number of missing values	6

5. NA16

Appendix Table A9 Fluorescence intensity and percent inhibition in each concentration of NA16.

Concentration (μM)	Log (conc.)	Fluorescence Intensity		Percent Inhibition	
		1	2	1	2
25.00000	1.398	56.96	44.52	76.10	71.68
12.50000	1.097	94.26	52.05	44.81	55.19
6.25000	0.796	75.82	44.62	60.28	71.46
3.12500	0.495	82.66	59.98	54.54	37.82
1.56250	0.194	88.86	64.57	49.34	27.77
0.78125	-0.107	93.83	59.8	45.17	38.22
0.39063	-0.408	122.48	67	21.14	22.45
0.19531	-0.709	101.21	66.06	38.98	24.51
0.09766	-1.010	87.14	67.77	50.79	20.77
0.04883	-1.311	112.88	63.08	29.19	31.04
0.02441	-1.612	109.55	71.51	31.99	12.58
0.01221	-1.913	107.46	71.02	33.74	13.65
0.00610	-2.214	111.92	76.19	30.00	2.33
0.00305	-2.515	111.06	73.65	30.72	7.89
0.00153	-2.816	115.58	76.43	26.93	1.80
0.00076	-3.118	103.18	71.22	37.33	13.21
0.00038	-3.419	144.34	74.24	2.80	6.60
0.00019	-3.720	127.89	66.5	16.60	23.55
0.00010	-4.021	112.22	77.06	29.75	0.42
0.00005	-4.322	107.52	73.62	33.69	7.96
0.00002	-4.623	109.01	73.21	32.44	8.85
0.00001	-4.924	115.67	71.87	26.85	11.79
No inhibitor	-	147.68	77.25	-	-

Appendix Table A10 Values from calculation of NA16 using Nonlinear regression curves to fit to three-parameter logistic equation.

Dose-response curve	Values
Best-fit values	
BOTTOM	22.34
TOP	91.95
LOGIC ₅₀	0.2317
IC ₅₀	1.705
Std. Error	
BOTTOM	3.357
TOP	11.17
LOGIC ₅₀	0.2639
95% Confidence Intervals	
BOTTOM	15.56 - 29.12
TOP	69.39 - 114.5
LOGIC ₅₀	-0.3014 - 0.7648
IC ₅₀	0.4995 - 5.819
Goodness of Fit	
Degrees of Freedom	41
R ²	0.6236
Absolute Sum of Squares	12672
Sy.x	17.58
Data	
Number of X values	22
Number of Y replicates	2
Total number of values	44
Number of missing values	0

6. NA17

Appendix Table A11 Fluorescence intensity and percent inhibition in each concentration of NA17.

Concentration (μM)	Log (conc.)	Fluorescence Intensity		Percent Inhibition	
		1	2	1	2
50.000	1.699	41.98	39.42	75.21	82.76
25.000	1.398	39.79	41.97	81.00	77.15
12.500	1.097	40.66	41.37	78.70	78.47
6.250	0.796	40.95	45.56	77.93	69.25
3.125	0.495	46.35	48.16	63.65	63.53
1.563	0.194	47.72	54.13	60.03	50.40
0.781	-0.107	50.01	55.8	53.97	46.72
0.391	-0.408	60.02	57.56	27.51	42.85
0.195	-0.709	56.53	61.35	36.74	34.51
0.098	-1.010	56.42	62.61	37.03	31.74
0.049	-1.311	59.02	71.69	30.15	11.76
0.024	-1.612	62.54	64.4	20.84	27.80
0.012	-1.913	62.56	66.96	20.79	22.17
0.006	-2.214	60.74	68.13	25.60	19.59
No inhibitor	-	70.42	77.03	-	-

Appendix Table A12 Values from calculation of NA17 using Nonlinear regression curves to fit to three-parameter logistic equation.

Dose-response curve	Values
Best-fit values	
BOTTOM	3.397
TOP	103.5
LOGIC ₅₀	0.0276
IC ₅₀	1.066
Std. Error	
BOTTOM	3.209
TOP	4.159
LOGIC ₅₀	0.09356
95% Confidence Intervals	
BOTTOM	-3.214 - 10.01
TOP	94.91 - 112.0
LOGIC ₅₀	-0.1651 - 0.2203
IC ₅₀	0.6837 - 1.661
Goodness of Fit	
Degrees of Freedom	25
R ²	0.9492
Absolute Sum of Squares	2169
Sy.x	9.315
Data	
Number of X values	14
Number of Y replicates	2
Total number of values	28
Number of missing values	0

APPENDIX B

Poster Contributions to Conferences

Poster Presentation to Conferences

- **Poster presentation: Inhibition of HIV-1 Reverse Transcriptase Activity with Dipyridodiazepinone Derivatives.**

Ratsupa Thammaporn, Kun Silprasit, Pornthip Boonsri, Supanna Techasakul, Kiattawee Choowongkomon and Supa Hannongbua. The abstract of 34th Congress on Science and Technology of Thailand (STT 34), Queen Sirikit National Convention Center, Bangkok, Thailand, October 31 – November 2, 2008



INHIBITION OF HIV-1 REVERSE TRANSCRIPTASE ACTIVITY WITH DIPYRIDODIAZEPINONE DERIVATIVES

Ratsupa Thammaporn^{1,2}, Kun Silprasit³, Pornthip Boonsri^{1,2}, Supanna Techasakul¹, Kiattawee Choowongkorn^{3,4} and Supa Hannongbua^{1,2,3}

¹Department of Chemistry, Faculty of Science, Kasetsart University, Bangkok 10900, Thailand.

²Center of Nanotechnology KU, Kasetsart University and NANOTEC Center of Excellence at Kasetsart University

³Interdisciplinary Graduated Program in Genetic Engineering, Kasetsart University, Bangkok 10900, Thailand.

⁴Department of Biochemistry, Faculty of Science, Kasetsart University, Bangkok 10900, Thailand.

Abstract

In this work, we reported the expression and purification of wild-type HIV-1 RT which was produced from recombinant bacteria. The yield of HIV-1 RT in culture 1 liter was 14.06 mg. Moreover, we studied effect of nevirapine and dipyrindodiazeponone derivative on the enzymatic activity of wild-type HIV-1 RT by using fluorometric measurement. The result shown that the IC₅₀ value of nevirapine inhibited wild-type HIV-1 RT with 0.74 μM, while the dipyrindodiazeponone derivatives, SPT/N16, SPT/NA14 and SPT/NA16 were 0.02, 0.016 and 0.0011 μM, respectively.

Introduction

HIV-1 reverse transcriptase (HIV-1 RT) is an important enzyme which catalyzes the conversion of single stranded RNA (ssRNA) into double stranded DNA (dsDNA). The active form of HIV-1 RT is a heterodimer that consists of 66 kDa and 51 kDa (p66 and p51). Nucleoside reverse transcriptase inhibitors (NRTIs) and non-nucleoside reverse transcriptase inhibitors (NNRTIs) are two classes of HIV-1 RT inhibitors which are used as a drug to inhibit HIV-1 RT. Moreover, NNRTIs have shown to be specific and less toxic than NRTIs. Currently, the new compounds of NNRTI are require to be developed and designed to effectively inhibit HIV-1 RT. In this work, we investigated the enzymatic activities of wild-type HIV-1 RT complexed with dipyrindodiazeponone derivatives by using fluorometric measurement with the PicoGreen reagent.

Methodology

The bacteria harboring such recombinant plasmid was cultured in Luria Bertani (LB) containing 100 μg/ml ampicillin and induced with isopropyl β-D-1-thiogalactopyranoside (IPTG) to express HIV-1 RT protein.

The expressed cells were lysed by sonication. And the protein in supernatant was precipitated with 50% ammonium sulfate.

The recombinant HIV-1 RT was purified by Phosphocellulose P11 and then DEAE cellulose column chromatography.

The enzymatic activities of wild-type HIV-1 RT and inhibitory efficiency of dipyrindodiazeponone derivatives were studied by a fluorometric method with the PicoGreen reagent.

Results and Discussion

From expression of the bacteria containing such recombinant plasmids of p51 and p66 was appeared as a major band. We could produce 14.06 mg of the heterodimer of HIV-1 RT from 1 liter of cell culture. Each step of expression and purification is shown in Figure 1 and Table 1.

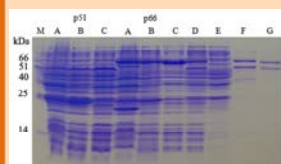


Figure 1: SDS-PAGE of each purification step of *E.coli* expressed HIV-1 RT. Maker (M), total cell lysate (A), soluble fraction (B), 50% ammonium sulfate (C), mixed p51 and p66 (D), unbounded (E) and bounded (F) fraction from P11 column and unbounded (G) fraction from DEAE column.

Table 1. Purification table and specific activity measured with the fluorometric method.

Fraction	Total protein (mg)	Fluorescence intensity (μg/μl)	Specific activity	Purification fold
Cell lysate	332.25	2.61	0.0078	1
Soluble fraction	309.64	2.56	0.0082	1.05
50% ammonium sulfate	93.71	2.60	0.02	3.53
P11 column	46.87	6.99	0.15	19.00
DEAE column	14.06	11.69	0.83	105.93

The dipyrindodiazeponone derivatives were tested against the HIV-1 RT activity. Each inhibitor, the IC₅₀ values were calculated from dose-response curves in the presence of increasing inhibitor concentrations. Nevirapine inhibited HIV-1 RT activity with IC₅₀ value of 0.74 μM. The IC₅₀ values of dipyrindodiazeponone derivatives were shown in Figure 2. The several of dipyrindodiazeponone derivatives including SPT/N14, SPT/N15, SPT/N16, SPT/NA14, and SPT/NA16 showed to have a higher IC₅₀ than Nevirapine and the SPT/NA16 was the highest IC₅₀ value among other derivatives.

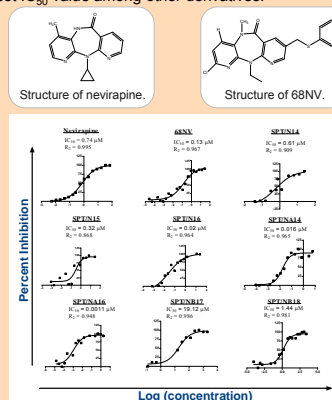


Figure 2: Effect of nevirapine, 68NV and dipyrindodiazeponone derivative on the enzymatic activities of wild-type HIV-1 RT.

Conclusion

We present the fluorometric assay method for quickly and accurately analysis of HIV-1 RT inhibitors and also identify a promising inhibitor, SPT/NA16, for further development.

References

- Singer, V. L., Jones, L. J., Yue, S. T., and Haugland, R. P. Anal. Biochem. 1997, 249, 228-238.
- Pata, J. D., Stirtan, W. G., Goldstein, S. W. and Steltz, T. A. PNAS. 2004, 101(29), 10548-10553.
- Khunnawutmanotham, N., et al. Molecules. 2007, 12, 218-230.

Acknowledgments

This research is supported by Thailand Research Fund (RTA5080005), the Postgraduate program in education and research on Petroleum, Petrochemical Technology and Advanced Materials, Ministry of Education, the Royal Golden Jubilee Ph.D. Program (PHD02622549) and National Synchrotron Research Center, Thailand.

CURRICULUM VITAE

NAME : Miss Ratsupa Thammaporn

BIRTH DATE : January 4, 1984

BIRTH PLACE : Bangkok, Thailand

NATIONALITY : Thai

EDUCATION	:	<u>YEAR</u>	<u>INSTITUTION</u>	<u>DEGREE/DIPLOMA</u>
		2002-2005	Kasetsart University	B.Sc. (Chemistry)
		2006-2009	Kasetsart University	M.Sc. (Chemistry)

SCHOLARSHIPS :

- 1) The Scholarship for Science Talented Students (full),
Comission on Higher Education (2002-2005)
- 2) Commission on Higher Education (National Center of
Excellence for Petroleum, Petrochemicals, and Advanced
Materials, NCE-PPAM) (2006-2008)
- 3) Thailand Research Fund (RTA5080005) (2009)
- 4) National Synchrotron Research Center, Thailand (2008)

PRESENTATION AND PUBLICATIONS

Thammaporn, R., K. Silprasit, P. Boonsri, S. Techasakul, K. Choowongkomon and S. Hannongbua. Inhibition of HIV-1 Reverse Transcriptase Activity with Dipyridodiazepinone Derivatives. The abstract of 34th Congress on Science and Technology of Thailand (STT 34), Queen Sirikit National Convention Center, Bangkok, Thailand, October 31 – November 2, 2008.

Silprasit, K., R. Thammaphorn, S. Hannongbua and K. Choowongkamon. 2008.

Cloning, Expression, Purification, Determining Activity of Recombinant HIV-1 Reverse Transcriptase. **Kasetsart J. (Nat. Sci.)** 42: 231-239.

Saparpakorn, P., R. Thammaphorn and S. Hannongbua. 2009. Use of 3D QSAR to

investigate the mode of binding of pyrazinones to HIV-1 RT. **Monatsh Chem** 140: 587-594.

Thammaphorn, R., K. Silprasit, S. Techasakul, K. Choowongkamon and S.

Hannongbua. Kinetic Study of HIV-1 Reverse Transcriptase Complexed with Inhibitors Based on Fluorometric Measurement, to be submitted.